COBALT-CATALYZED KUMADA COUPLING AND THE DEVELOPMENT OF A CC LIGAND AND METALATION TO COBALT

BY

JACK KILLION

THESIS

Submitted in partial fulfillment of the requirements
for the degree of Master of Science in Chemistry
in the Graduate College of the
University of Illinois at Urbana-Champaign, 2017

Urbana, Illinois

Advisor:

Assistant Professor Alison R. Fout

ABSTRACT

Inspired by work in our group using low-coordinate Co(I) complexes for amination of aryl halides, a $Co(acac)_3$/PN precatalyst was developed and optimized for catalytic Kumada coupling of aryl Grignard reagents to sterically encumbered alkyl halides. The substrate scope demonstrates excellent yields for primary alkyl chlorides and bromides, including good performance using neopentyl chloride and neophyl chloride. Secondary alkyl halides were successfully arylated in good yields as well, and the presence of β-hydrogens in a substrate did not inhibit product formation. An intermolecular functional group tolerance screen was conducted which indicates that ester and amide functionality are well tolerated by the reaction conditions. Electrophiles containing ester, pyridine, and nitrile functionality were all coupled with 2-mesitylmagnesium bromide in good yields, supporting tolerance screen results. The intermolecular screen also showed that functional groups which are typically reactive with Grignard reagents such as alcohols and terminal alkynes were not well tolerated by the reaction.

A series of bidentate CC ligands were developed featuring an anionic C_{aryl} and *N*-heterocyclic carbene (NHC) coordination to provide an electron rich, strong field ligand environment and promote novel reactivity by first-row transition metals. These ligands were treated with various cobalt sources to attempt to coordinate the NHC and affect C_{aryl}–Br activation to produce the desired bidentate complexes. However, four coordinate cobalt(II) complexes binding at the NHC of two ligands and two halides were preferentially formed, limiting the applicability of this ligand.

ACKNOWLEDGEMENTS

I'd like to give special thanks to the members of my research group, past and present: Ellen, Marshall, Zack, Yun Ji, Abdul, Gabe, Kenan, Bailey, Courtney, Michael, Joe, Tabitha, and Safiyah. You all have been wonderful collaborators and friends and commiserators. Abdul, Gabe, and Kenan were particularly important to my grad school experience, serving as mentors and giving me invaluable advice and discussion. To my Adviser, Alison Fout, who helped me grow as a student and as a scientist and gave me the tools that I will carry forward into a professional career.

More than anyone I need to thank Ben, Marla, Max, and Beth, my family. Without your support I certainly wouldn't have made it to the place I am today. As I'm writing this, I'm being regaled over group text with some anecdote about the dogs. To my friends here and afar, who helped to make those few hours outside of lab more enjoyable. And lastly, I would be remiss not to thank Madi Stalzer, who gave me advice and support at times that I sorely needed it, and helped me grow as a person in ways I'm sure she doesn't realize.

TABLE OF CONTENTS

CHAPTER 1: INTRODUCTION

Transition metal coordination chemistry and its applicability to catalytic transformation of organic compounds has been a topic of great interest for decades, spurring innovation broadly across the industrial and academic sectors of chemical research. Traditionally, second- and third-row late transition metals such as Pd, Pt, Rh, and Ir have been the workhorses of homogeneous metal catalysis due to their dependable and consistent reactivity.[1] Palladium in particular has long occupied a dominant role, owing to the powerful +0/+2 oxidation state couple that drives reliable oxidative addition and reductive elimination pathways.[2] This has led to the development of catalysts which can activate inert chemical bonds and execute challenging bond forming reactions while minimizing engagement in deleterious side reactions. However, use of the aforementioned metals to mediate large scale chemical syntheses can present substantial practical issues. High toxicity of heavier elements requires strict regulations for purification to minimize metal concentration in finished products, especially in pharmaceuticals, and contaminated waste can be hazardous to the environment.[3] Additionally, many palladium catalyzed reactions require the use of exotic phosphine ligands which are frequently even more costly than the metals themselves.[4] For these reasons, much recent work has been invested in exploration of catalysis using first-row transition metals.[5-7]

So-called base metals such as iron, cobalt and nickel are significantly more Earth abundant than their second- and third-row congeners, meaning their implementation in large-scale syntheses could result in substantially reduced operating cost. For instance, while nickel costs about $1/g, fellow d^{10} metals palladium and platinum are $183/g and $483/g, respectively.[8] In theory, first-row metals are capable of even greater reaction rates than corresponding second-row metals due to greater density of states, which has been cited as the reason for greater performance of the second-row over the third.[9] Despite these potential advantages though, first-row metal catalysts continue to lag behind palladium and other heavy elements in the chemical

industry. This is in part due to propensity of first-row metals to preferentially undergo one-electron redox events over concerted two-electron oxidative addition or reductive elimination pathways in most cases, standing in contrast to their second- and third-row congeners. The result of this is involvement of uncaged radical transformations in the mechanism of many first-row metal-catalyzed reactions; this can lead to more complex product distributions due to side reactions, and often a need for a higher catalyst loading, tempering the potential financial benefits of employing them in place of palladium. Therefore, the necessary path to developing more effective first-row metal catalysts involves harnessing this potentially advantageous reactivity and employing it in a more controllable fashion.

One of the core strategies for fostering interesting reactivity using first-row transition metals is the use of a strong-field ligand environment. Compression of the metal d-orbitals by strongly overlapping ligands increases orbital energy splitting, forcing the metal center into a low-spin electronic state, which has been shown to promote two-electron reaction pathways more closely resembling the properties of second-row metals. For this purpose, ligands employing coordination to carbon or phosphorous are effective due to orbital energy close to the d-orbitals of iron, cobalt and nickel, resulting in excellent orbital overlap.

The following chapters describe efforts to employ these strong-field ligand approaches to promote unique and desirable reactivity by cobalt. Cobalt catalysis has in many cases garnered less attention than that of nickel or iron, though its cost and toxicity are comparable. Carbon-carbon formation reactions mediated by cobalt have been shown to enjoy similarly high yields as compared to nickel- and palladium- catalyzed methods, and with differing substrate scope. Decomposition by β-hydride elimination is not as present an issue for cobalt as the d^{10} metals, opening up a range of more accessible cobalt-alkyl catalytic intermediates.[11] Thus, development of a method of efficient carbon-carbon bond formation using inexpensive cobalt/ligand combinations is highly desirable.

The emergent field of coordination chemistry involving *N*-heterocyclic carbene (NHC) ligands has also attracted a great deal of interest. The Fout group has recently reported cobalt complexes using a monoanionic bis(carbene) ligand platform which have demonstrated applicability towards hydrogenation of internal alkynes[12] as well as anti-Markovnikov hydrosilylation of terminal olefins.[13] However, investigation of metal complexes featuring bidentate CC ligands is relatively underrepresented in the literature. Development of a new bidentate CC ligand and its interaction with cobalt are detailed within.

1.1 References

1. Marion, N.; Nolan, S. P. Well-Defined *N*-Heterocyclic Carbenes—Palladium(II) Precatalysts for Cross-Coupling Reactions. *Acc. Chem. Res.* **2008**, *41* (11), 1440-1449.
2. Jana, R.; Pathak, T. P.; Sigman, M. S. Advances in Transition Metal (Pd, Ni, Fe)-Catalyzed Cross-Coupling Reactions Using Alkyl-organometallics as Reaction Partners. *Chem. Rev.* **2011***, 111*, 1417-1492.
3. Magano, J.; Dunetz, J. R. Large-Scale Applications of Transition Metal-Catalyzed Couplings for the Synthesis of Pharmaceuticals. *Chem. Rev.* **2011**, *111*, 2177-2250.
4. Nelson, D. J.; Nolan, S. P. In *Contemporary Catalysis*; The Royal Society of Chemistry: London, UK, 2017; pp 396–401.
5. Brennan, M. R., Kim, D., Fout, A. R. A Synthetic and Mechanistic Investigation into the Cobalt(I) Catalyzed Amination of Aryl Halide. *Chem*. *Sci*. **2014**, *5*, 4831-4839.
6. Tasker, S. Z.; Standley, E. A.; Jamison, T. F. Recent Advances in Homogeneous Nickel Catalysis. *Nature.* **2014**, *509*, 299-309.
7. Chirik, P. Morris, R. Getting Down to Earth: The Renaissance of Catalysis with Abundant Metals. *Acc. Chem. Res.* **2015**, *48*, 2495.
8. Su, B.; Cao, Z. C.; Shi, Z. J. Exploration of Earth-Abundant Transition Metals (Fe, Co, and Ni) as Catalysts in Unreactive Chemical Bond Activations. *Acc. Chem. Res.* **2015**, *48*, 886-896.
9. Volpe, E. C.; Manke, D. R.; Bartholomew, E. R.; Wolczanski, P. T.; Lobkovsky, E. B. Aryl—Oxazoline Chelates of First-Row Transition Metals: Structures of {*κ-C,N*-(*o*-C_6H_4)CMe_2($COCH_2CMe_2N$)}FeCl(py) and [{*κ-C,N*-(*o*-C_6H_4)CMe_2($COCH_2CMe_2N$)}Cr(*μ*-Cl)]$_2$. *Organometallics.* **2010**, *29*, 6642-6652.
10. Banno, T.; Hayakawa, Y.; Umeno, M. Some Applications of the Grignard Cross-Coupling Reaction in the Industrial Field. *J. Organomet. Chem.* **2002**, *653*, 288-291.
11. Cahiez, G.; Moyeux, A. Cobalt-Catalyzed Cross-coupling Reactions. *Chem. Rev.* **2010**, *110*, 1435-1462.
12. Tokmic, K.; Markus, C. R.; Zhu, L.; Fout, A. R. Well-Defined Cobalt(I) Dihydrogen Catalyst: Experimental Evidence for a Co(I)/Co(III) Redox Process in Olefin Hydrogenation. *Journal of the American Chemical Society* **2016**, *138* (36), 11907.
13. Ibrahim, A. D.; Entsminger, S. W.; Zhu, L.; Fout, A. R. A Highly Chemoselective Cobalt Catalyst for the Hydrosilylation of Alkenes Using Tertiary Silanes and Hydrosiloxanes. *ACS Catalysis* **2016**, *6* (6), 3589.

CHAPTER 2: FORMATION OF STERICALLY ENCUMBERED C–C BONDS MEDIATED BY A $CO(ACAC)_3$/PN PRECATALYST

2.1 Introduction

Metal-catalyzed cross-coupling to create carbon-carbon bonds is a widely studied field which has fostered a great deal of innovation in a diverse number of chemical synthetic methods. While C–C bond-forming reactions are largely the domain of palladium catalysis,[1] there is a growing interest in employing first-row transition metals to catalyze these transformations. In addition to being less costly and more environmentally benign, first-row metals in the appropriate ligand environment offer reactivity that is comparable to that of second- and third-row metals but often orthogonal in scope. In the context of C–C bond construction, first row metals are best represented in the coupling of organomagnesium compounds and alkyl or aryl halides, broadly known as Kumada-Corriu coupling.

One of the main challenges associated with Kumada coupling is bond formation involving highly sterically encumbered groups. Biscoe has recently reported nickel-catalyzed coupling of aryl halides with *tert*-butylmagnesium bromide in good yields,[2] though performance decreases dramatically in the case of *ortho*-substitution on the electrophile. Installation of neopentyl groups by cross-coupling is even less common, often requires catalyst systems that are highly air sensitive, and may represent a challenge when applying to large-scale or industrial synthesis.[3] The neopentyl group on a polymer side chain has been shown to affect bulk properties,[4] and quaternary carbons can influence binding affinity of potential pharmaceutical therapies in biological media,[5] making facile installation of quaternary centers an attractive synthetic tool.

Cobalt-catalyzed C–C bond formation using Grignard reagents was first described by Karasch in 1941,[6] who was able to expand the method to alkenylation of PhMgBr using vinyl

halides.[7] Since then, Kumada type cross-coupling with cobalt has been studied extensively; methods most commonly employ $CoCl_2$ or another cobalt(II) salt and a chelating ligand such as *N,N,N',N'*-tetramethylethylenediamine (TMEDA) or 1,2-(bis-diphenylphosphino)ethane (dppe), and demonstrate strong performance for both sp^2-sp^2 and sp^2-sp^3 bond formation.[8] However, much like nickel- and palladium-catalyzed Kumada coupling, cobalt has historically struggled with substrates bearing large steric profiles, particularly in the case of aliphatic halides.

2.2 Catalyst Development

Our group has previously reported cobalt-catalyzed amination of aryl halides using sterically bulky amide coupling partners.[9] These results led us to target cobalt systems that could be used to facilitate the formation of carbon-carbon bonds in highly encumbered environments as well. However, use of even our most active catalyst for C–N bond formation, (dppf)$CoN(SiMe_3)_2$, (dppf = 1,1'-(bis-diphenylphosphino)ferrocene) resulted in <10% yield of cross-coupled product when bulky alkyl nucleophiles such as neopentylmagnesium chloride were used instead. Recent work by Cahiez[10] and Oshima[11] have demonstrated that bidentate amine ligated $Co(acac)_3$ is an effective precatalyst system for some Kumada type cross-coupling reactions, hypothesizing the involvement of an active Co(I) species in the mechanism.

Use of $Co(acac)_3$ as a precatalyst is an attractive option owing to its relative stability and ease of storage, making it ideal for a wide swath of applications for which it can be prohibitive to use catalysts that are highly sensitive or difficult to synthesize. With this goal in mind, we explored a range of bidentate ligand additives to access carbon-carbon bond formation of highly encumbered substrates (**Figure 2.1**). Bidentate amine ligands such as TMEDA performed well in cross-coupling 2-mesitylmagnesium bromide (MesMgBr) with isopropyl bromide, in good corroboration with earlier reports, but failed to furnish the cross-coupled product with neopentyl

halides. A bis-phosphine additive such as dppf resulted in as much as 33% formation of neopentylmesitylene but was overall less effective at coupling less encumbered electrophiles than TMEDA. We reasoned then that a ligand of mixed donor strength might be able to retain the good steric tolerance observed with bidentate phosphines while bolstering yields like with TMEDA. Inclusion of one such ligand, *N*,*N*-dimethyl-2-(diphenylphosphino)aniline (PN), in the reaction resulted in cross-coupling of MesMgBr to isopropyl bromide at 93% yield and to neopentyl chloride at 71% yield, a substantial improvement over both bis-phosphine and bis-amine ligands.

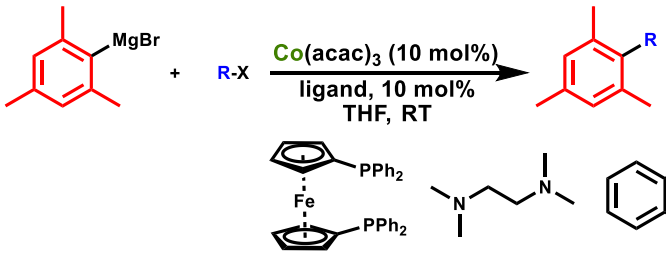

R-X		dppf	TMEDA	P-N
^{i}Pr-X	X=Cl	59%	0%	88%
	X=Br	65%	95%	93%
Np-X	X=Cl	25%	0%	71%
	X=Br	33%	0%	86%

Figure 2.1: Ligand optimization.

It appears that numerous cobalt species can be applied to Kumada coupling of relatively unhindered substrates (**Table 2.1**). $CoCl_2$, $Co(acac)_2$, and $(PN)CoMes_2$ all couple MesMgBr and benzyl bromide in good yields. However, none of those are capable of coupling MesMgBr with a more challenging substrate such as neophyl chloride. Additionally, control experiments using only PN ligand or Na(acac) and PN furnished no cross-coupled product, confirming that inclusion of cobalt was necessary for the reaction to proceed, and that any magnesium species formed were not primarily responsible for product formation.

Table 2.1: Kumada coupling control experiments.

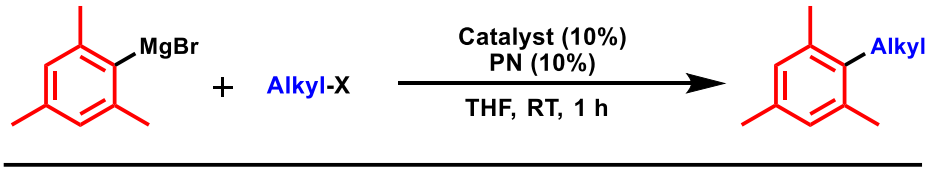

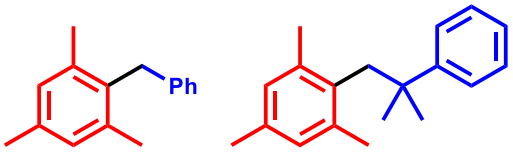

Catalyst	Yield	Yield
$Co(acac)_3$	98%	70%
$CoCl_2$	96%	not formed
$Co(acac)_2$	95%	not formed
$(PN)CoMes_2$	89%	not formed
$Co_2(CO)_8$	94%	not formed
Na(acac)	<5%	not formed
none	<5%	not formed

2.3 Results and Substrate Scope

MesMgBr and 1,3,5-triisopropylphenylmagnesium bromide (TRIPMgBr) were selected as nucleophiles and coupled to a series of electrophiles across a range of steric profiles (**Table 2.2**) to assess the performance of the $Co(acac)_3$/PN precatalyst system. Benzyl bromide could be coupled to both nucleophiles in near quantitative yields, and a neopentyl group could be installed on the TRIP moiety in as much as 72% yield, though it is worth noting that reactions using TRIPMgBr proceeded best with additional Grignard reagent and a longer reaction time. Secondary alkyl halides were also well tolerated, with high yields using both isopropyl bromide

and cyclohexyl bromide. Of particular note is neophyl chloride, which could be coupled to both MesMgBr and TRIPMgBr in good isolated yields 70% and 66%, respectively.

Table 2.2: Substrate table of Kumada coupling.

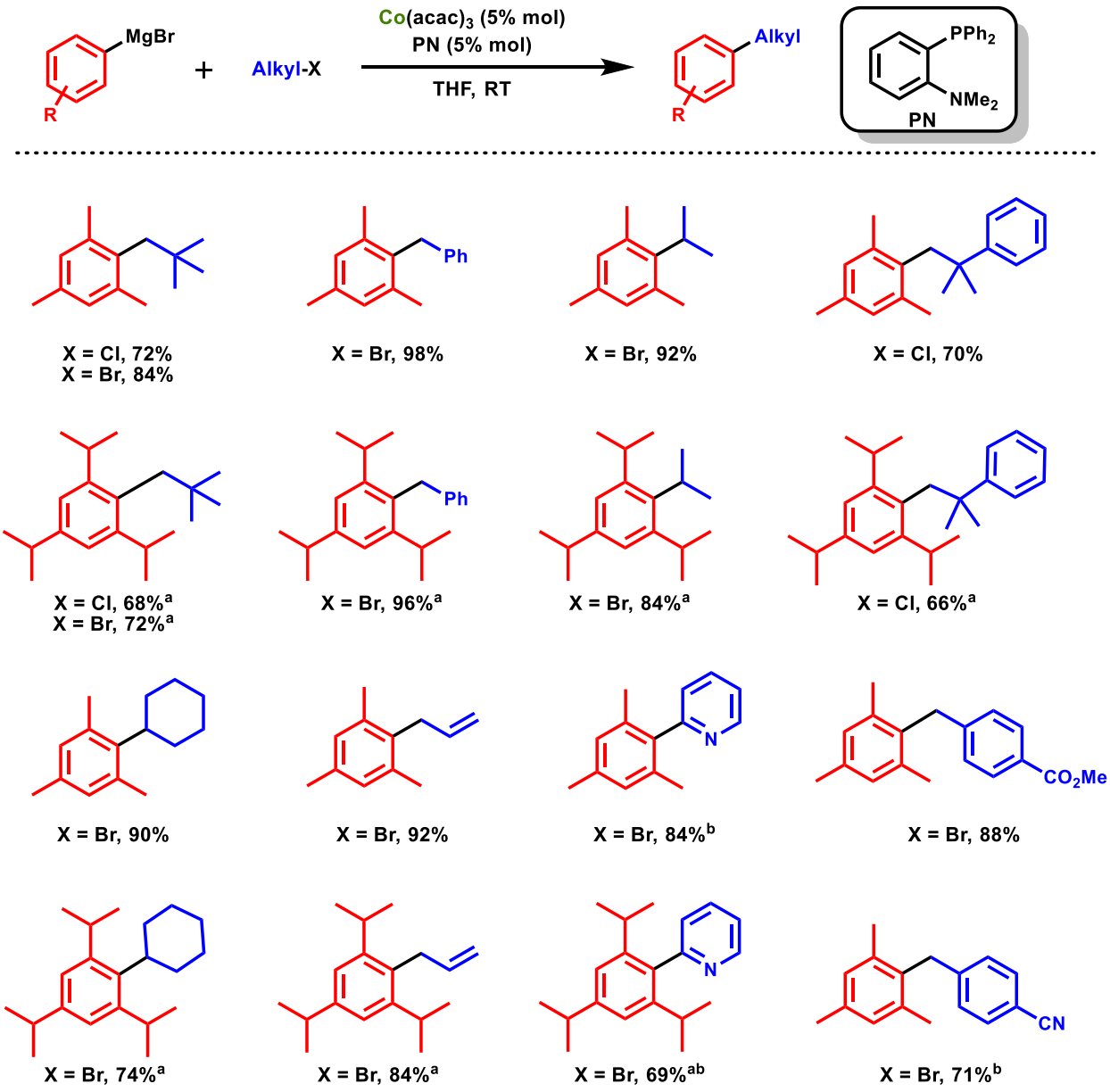

[a]2 eq. TRIPMgBr used, and stirred for 16 h
[b]C_6H_6 used as solvent instead of THF

Assessment of functional group tolerance for the reaction conditions was adapted from an intermolecular robustness screen method developed by Glorius and coworkers.[12] A traditional substrate scope for a particular reaction involves acquisition or synthesis of bifunctional substrates to approximate the influence of various functional groups on catalyst performance as would be observed in a synthetic application. This often gives valuable qualitative information on applicability of a catalytic system in synthesis. However, such a method is often highly time- and labor-intensive, and does not differentiate between a functional group's steric and/or electronic influence on a reaction versus its stability toward the catalyst system and general reaction environment.

The intermolecular robustness screen is performed by choosing a high-yielding model reaction, evaluating performance in the presence of an additive compound in equimolar quantity to substrate which bears functionality of interest. Both product yield and quantity of additive remaining are then monitored over time. In short, a given functional group is considered to be tolerated well by the conditions if the reaction results both in high yield of cross-coupled product and little to no consumption or decomposition of additive. By this method, the tolerance of a large number of functional groups can be assessed for a reaction in a short time, using inexpensive and readily obtained reagents, and a functional group's steric/electronic influence is decoupled from its stability under reaction conditions. The method does not give information on the specific electronic effects of a functional group in the way of a traditional substrate scope. This method has been applied by Mankad,[13] Szymczak,[14] and others since its initial publication for assessment of functional group tolerance. It is worth noting that the original Glorius method calls for examination of leftover starting material as well, but alkyl halides did not appear to participate in side reactions to any significant degree during the reactions, and the high reactivity of Grignard reagents make it difficult to ascertain whether decomposition of nucleophile occurs during the reaction or in the process of data collection.

Table 2.3: Results of the intermolecular tolerance screen.

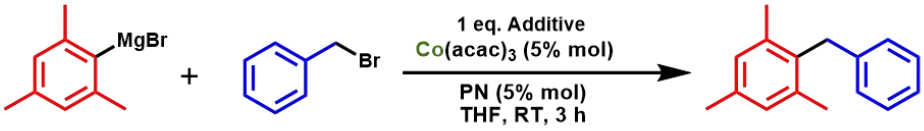

Additive	Product Yield	Additive remaining	Additive	Product Yield	Additive remaining
No Additive	97%	--	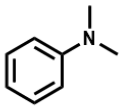	54%	50%
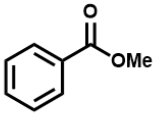	92%	91%	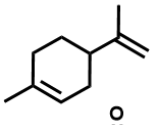	55%	95%
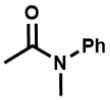	70%	93%	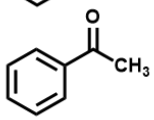	35%	77%
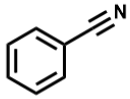	77%	24%	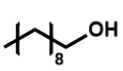	3%	48%
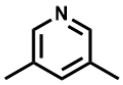	96%	29%	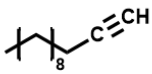	23%	24%

99-67% 66-34% 33-0%

Benzyl bromide and MesMgBr were chosen as model substrates for the intermolecular screen (**Table 2.3**). Ester and amide functionality were well tolerated, resulting both in good to high yields and good retention of the additive. Additives featuring good sigma-donors were typically consumed under reaction conditions, though with low to moderate inhibition of product formation. Introduction of 3,5-lutidine did not inhibit formation of product, but only 29% remained in solution after the reaction, suggesting that it may be participating as a ligand to cobalt during catalysis and/or participating in side reactions. Also notable is the influence of olefin functionality on the reaction; introduction of d-limonene on the reaction resulted in significant inhibition of cross-coupling, but little to no loss of additive. Protic functionality resulted in substantial inhibition

of product formation, as did introduction of a ketone, as is to be expected due to reactivity of those groups with Grignard reagents.

Select results of the intermolecular screen were evaluated by comparison to catalytic performance on substrates with the corresponding functional groups. A methyl ester-substituted benzyl bromide was coupled to MesMgBr at 88% yield under catalytic conditions, in good agreement with the intermolecular screen. Introduction of Lewis basic functionality was also well tolerated, demonstrating that the loss of additive observed in the above tolerance screen did not correspond to greatly diminished yield when such groups are present.

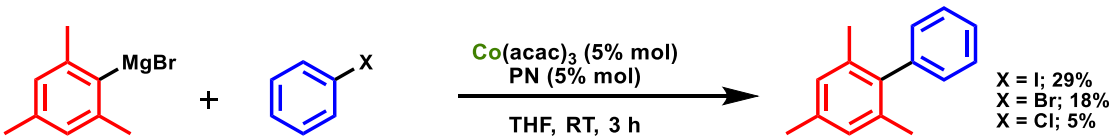

Scheme 2.1: Kumda coupling using aryl electrophiles.

While high activity was demonstrated toward Kumada coupling of aryl nucleophiles with alky halides, the $Co(acac)_3$/PN catalyst system failed to furnish comparable results with aryl halide electrophiles. Phenylmesitylene could be formed in as much as 29% yield from MesMgBr and iodobenzene, and fell to less than 5% when chlorobenzene was used (**Scheme 2.1**). Performance also suffered for tertiary alkyl halides such as *tert*-butylbromide and the secondary halide 1-(bromoethyl)benzene, though the latter case may be due in part to susceptibility of the substrate to radical side reactions. Reaction of MesMgBr with 1,2-dibromoethane resulted in only trace production of monocoupled 2-(2-bromoethyl)-mesitylene and no evidence of two successive arylations at one substrate. Further investigations on dihalogenated substrates were not conducted.

A brief survey of nucleophile tolerance was also conducted. While arylmagnesium halides were generally well tolerated, no cross-coupled product was observed when vinylmagnesium

bromide was reacted with neophyl chloride or benzyl bromide. Alkyl Grignard reagents such as *tert*-butylmagnesium chloride and ethylmagnesium bromide were each coupled with benzyl bromide in less than 10% yield. Use of 2-mesityllithium as a nucleophile resulted in no observable cross-coupled product with any substrate attempted; this result is unsurprising given the few examples of organolithium reagents used for cross-coupling relative to their organomagnesium counterparts.[15]

Table 2.4: Additional substrates attempted.

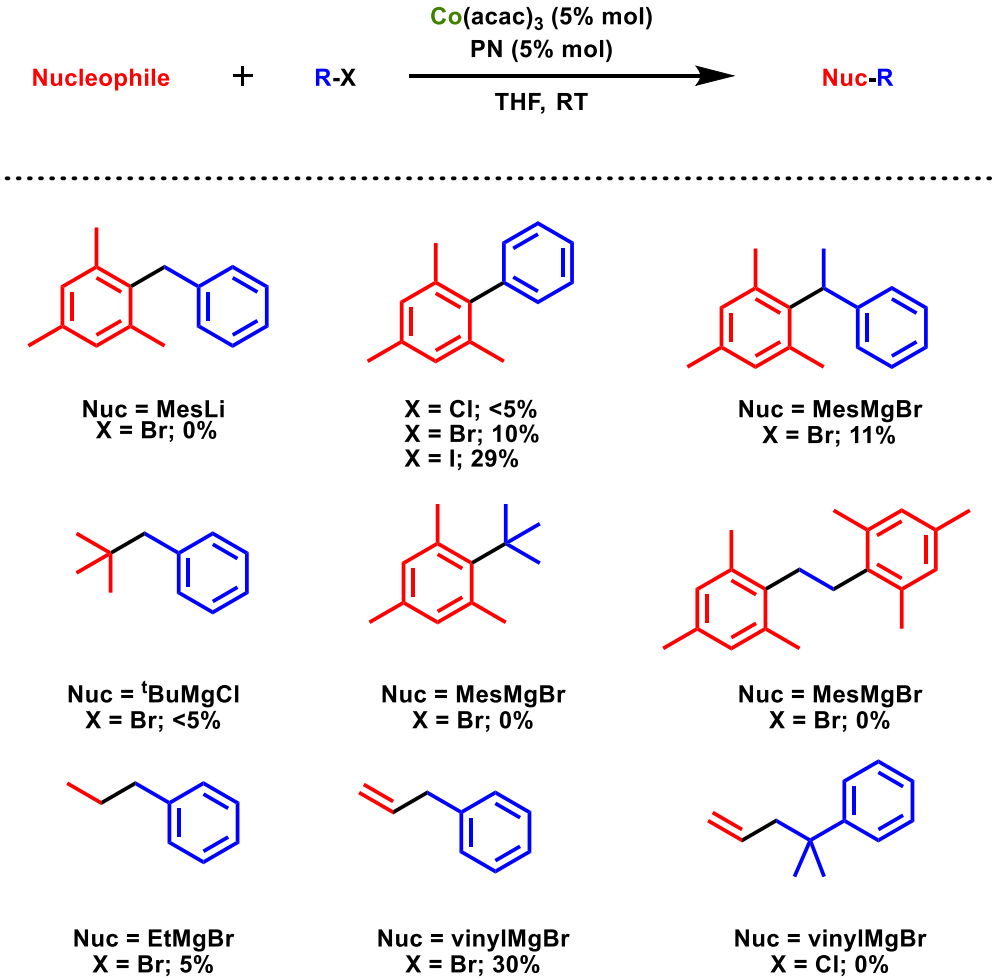

2.4 Mechanistic Study

In order to gain insights into the operating mechanism in this reaction, various control experiments were performed. The precatalyst $Co(acac)_3$ was unreactive towards stoichiometric amounts of each the PN ligand and benzyl bromide, as well as a combination of the two. This would suggest that catalysis does not initiate until introduction of the Grignard reagent. Reaction of $Co(acac)_3$ with 1-3 equivalents of MesMgBr generally resulted in a ^1H NMR spectrum suggesting a mix of paramagnetic products which resisted further characterization. Additionally, this mix of species was not able to effectively catalyze C–C bond coupling, indicating formation of decomposition products rather than a potential active catalyst.

Treatment of a benzene solution containing both $Co(acac)_3$ and PN with three equivalents of MesMgBr resulted in clean formation of a single paramagnetic species. Observation of bimesityl in the reaction mixture suggested that cobalt was reduced by MesMgBr, likely either to a Co(I) species by reductive elimination or a Co(II) species by intermolecular or radical process. This bright orange complex was capable of coupling benzyl bromide and MesMgBr, yielding as high as 89% benzylmesitylene. However, a substantially diminished yield was observed when more challenging substrates such as neophyl chloride were used implying that this species may not be catalytically relevant in those transformations.

In order to conclusively determine the identity of the orange paramagnetic product, crystals suitable for X-ray diffraction were grown from concentrated hexanes. Structural refinement of the data revealed the cobalt(II) species $(PN)CoMes_2$ (**Figure 2.2**). It is likely that this complex is formed by one electron reduction of $Co(acac)_3$ followed by coordination of the PN ligand as well as transmetallation of two mesityl groups to the cobalt center; however, the precise mechanism of the reaction remains uncertain. Formation of this complex under the above conditions could indicate that the catalytic cycle proceeds by a mechanism involving single

electron oxidation/reduction events, as is commonly observed in cobalt-catalyzed cross-coupling and specifically in examples of Kumada coupling mediated by other first-row transition metals such as nickel (**Figure 2.3**).[16]

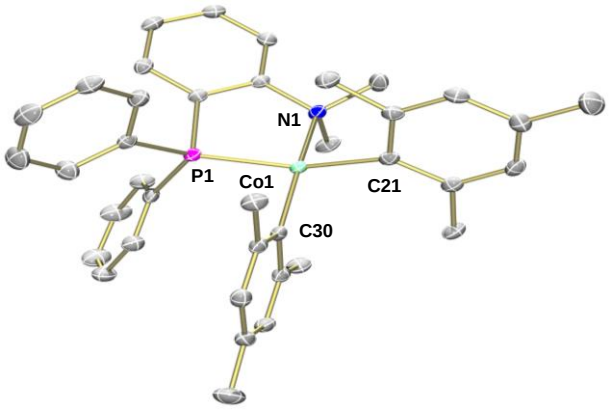

Figure 2.2: X-ray crystal structure of (PN)$CoMes_2$ depicted with 50% probability ellipsoids. Solvent molecules and H atoms have been omitted for clarity. Selected bond distances (Å) and angles (°): Co1–N1 2.1956(17), Co1–P1 2.2106(6), Co1–C21 1.976(2), Co1–C30 1.944(2), N1–Co1–P1 83.72(5), C21–Co1–P1 160.14(6), C21–Co1–N1 95.05(7), C30–Co1–P1 92.63(6), C30–Co1–N1 159.45(8), C30–Co1–C21 95.08(8).

Further stoichiometric coupling experiments were conducted using pre-generated (PN)$CoMes_2$ in hopes of assessing its role in the mechanism of the reaction. Coupling benzyl bromide and MesMgBr using pre-generated (PN)$CoMes_2$ at 10 mol% catalyst loading resulted in formation of cross-coupled product at 89% yield, as compared to 98% using the $Co(acac)_3$/PN

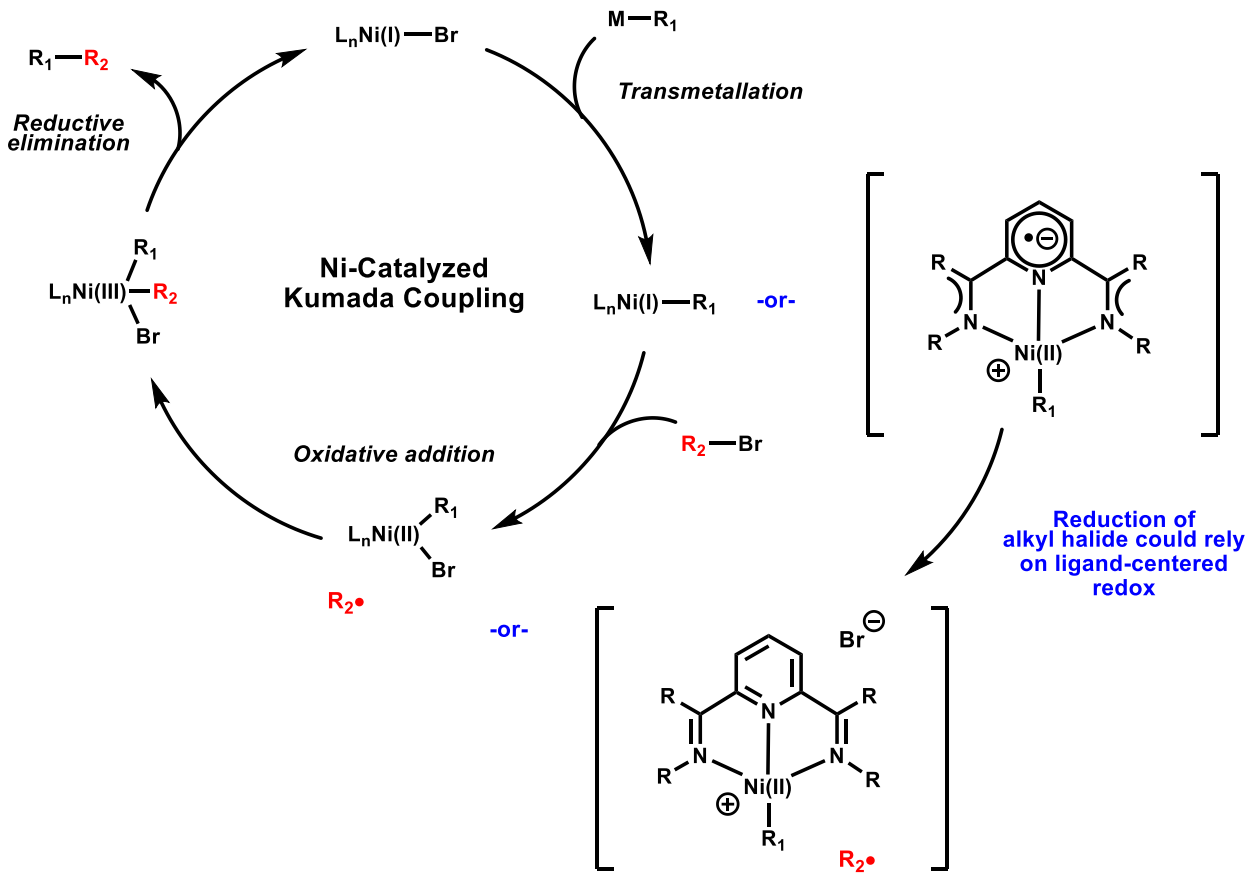

Figure 2.3: Proposed Mechanism of Ni-Catalyzed Kumada Coupling (adapted from ref 16).

precatalysts. This loss of performance could be due to instability of the catalyst; however, the same reaction using (PN)$CoMes_2$ in an equimolar quantity relative to substrate did not improve upon this yield. Additionally, reaction of MesMgBr with neopentyl chloride furnished 30% product formation at 10% (PN)$CoMes_2$ (compared to 72% under standard conditions), but less than 5% with equimolar (PN)$CoMes_2$. These findings indicate that the (PN)$CoMes_2$ species is not an active species in the mechanism of the catalysis, but more likely a side product which forms in the absence of electrophile. This complex may then react with additional Grignard reagent to form a more catalytically relevant species, perhaps resulting in the observed reduction of yield when the quantity of (PN)$CoMes_2$ is increased relative to MesMgBr.

Involvement of a lower valent cobalt species in the catalysis was also investigated. There are numerous examples of oxidative addition of R–X bonds by Co(0) complexes to support potential involvement of such a species in this system.[17] While the dimeric Co(0) complex $Co_2(CO)_8$ was unreactive towards PN likely due in part to its coordinative saturation by strongly coordinating CO ligands, it was capable of coupling MesMgBr and benzyl bromide in 67% yield at 10% catalyst loading and 94% with 1 equiv. additive of PN relative to cobalt. However, this complex again failed to handle more challenging electrophiles such as neopentyl chloride. It is worth noting that the presence of carbonyl ligands offers a significantly different coordination environment than what might be generated under standard catalytic conditions. Though a Co(0) species is likely capable of breaking the necessary carbon-halide bonds in catalysis, a radical mechanism involving cobalt in the +1 and +2 oxidation states is more probable. The exact role of the $Co(acac)_3$ and PN combination in the coupling of highly bulky substrates is as yet uncertain.

2.5 Summary

In summary, $Co(acac)_3$ demonstrates high performance in the catalytic construction of C–C bonds in highly sterically encumbered environments when paired with the mixed-donor PN ligand additive. Installation of quaternary centers on bulky organic substrates has been demonstrated, and the conditions offer functional group tolerance comparable to typical methods of Kumada-Corriu cross-coupling. This method has potential for application towards syntheses which require installation of neopentyl or other similarly challenging groups using materials that are inexpensive and easily handled. The inclusion of both $Co(acac)_3$ and PN both appear to be vital to achieve such high yields among the more challenging substrates, though the precise role of these specific precatalysts to accomplish such unique reactivity is as yet uncertain; further mechanistic investigation may be warranted.

2.6 Experimental

2.6.1 General Considerations

All manipulations of metal complexes were carried out in the absence of water and dioxygen using standard Schlenk techniques, or in an MBraun inert atmosphere drybox under a dinitrogen atmosphere except where otherwise specified. All glassware was oven dried for a minimum of 8 h and cooled in an evacuated antechamber prior to use in the drybox. Diethyl ether, tetrahydrofuran, toluene and benzene were dried and deoxygenated on a Glass Contour System (SG Water USA, Nashua, NH) and stored over 4 Å molecular sieves (Strem) prior to use. Chloroform-*d* and Benzene-d_6 were purchased from Cambridge Isotope Labs and were degassed and stored over 4 Å molecular sieves prior to use. Cobalt *tris*(acetylacetonate) was purchased from Strem and used as received. Dppf was purchased from AOKChem (>99%) and used as received. Alkyl halides were purchased from Sigma-Aldrich and used without further purification. Mesitylmagnesium bromide and triisopropylphenylmagnesium bromide were purchased from Sigma-Aldrich as solutions in THF and used as received. Aminophosphine ligands were prepared according to literature precedent; an optimized procedure for the synthesis of *N*,*N*-dimethyl-2-(diphenylphosphino)aniline (PN) is presented below. Celite® 545 (J. T. Baker) was dried in a Schlenk flask for 24 hr under dynamic vacuum while heating to at least 150˚C prior to use in a drybox. NMR Spectra were recorded at room temperature on a Varian spectrometer operating at 500 MHz (^{1}H NMR) and 126 MHz (^{13}C NMR) and referenced to the residual $CHCl_3$ or C_6H_6 resonance (δ in parts per million, and *J* in Hz); ^{31}P Spectra were collected at 200 MHz and referenced to an external standard of H_3PO_4. Mass spectrometry (MS) was performed by the University of Illinois Mass Spectrometry Laboratory. Electron Impact (EI) spectra were performed at 70 eV using methane as the carrier gas on a Finnegan-MAT C5 spectrometer. Data are reported in the form of m/z (intensity relative to the base peak = 100).

2.6.2 Optimized Synthesis of PN Ligand

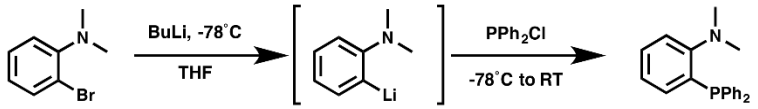

2-Bromo-(N,N-dimethyaniline) (2.06 g, 10.3 mmol) is taken up in degassed THF (17 mL) under N_2 in a 100 mL round bottom flask. The reaction mixture is cooled to -78°C and stirred as n-BuLi (1.6 M in hexane, 6.8 mL, 10.86 mmol, 1.05 eq.)is added dropwise. The reaction mixture is stirred at -78°C for 30 minutes, then warmed to 0°C and stirred for 15 minutes. Following this, the reaction is cooled back down to -78˚C and PPh_2Cl (1.93 mL, 10.86 mmol, 1.05 eq.) is added dropwise over three minutes. The resulting reaction mixture was warmed to 0°C and stirred for two hours before allowing the reaction to warm to room temperature slowly overnight. The resulting crude mixture was then filtered over a pad of Celite® and concentrated. The residue was filtered over silica gel, eluting with 10% ethyl acetate/hexanes; the resulting solution was cooled to 8˚C, resulting in the crystallization of the desired product as a white solid.

^{1}H NMR (500 MHz, Chloroform-*d*) δ 7.36 – 7.27 (m, 10H), 7.21 (ddd, J = 8.1, 4.8, 1.2 Hz, 1H), 7.00 (td, J = 7.5, 1.2 Hz, 1H), 6.80 (ddd, J = 7.6, 3.8, 1.6 Hz, 1H), 2.61 (s, 6H); ^{13}C NMR (126 MHz, Chloroform-*d*) δ = 158.3, 138.4, 134.6, 134.5, 134.0, 130.0, 128.54, 128.4, 124.6, 120.7, 45.7; ^{31}P NMR (202 MHz, Chloroform-*d*) δ -13.24.

2.6.3 Representative Procedure for the Alkylation of Organomagnesium Halides

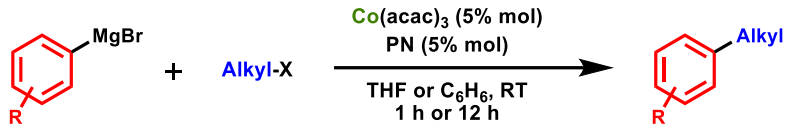

Note: The reactions described in this work were carried out in an air-free glovebox. However, the reactions can be carried out in vials on the bench top without rigorously dried solvent, so long as the headspace is purged with dinitrogen prior to the addition of the organomagnesium halide and sealed promptly. Under these conditions, isolated yields were essentially identical to those run in a glovebox.

Representative procedure. Alkyl halide (1 mmol), cobalt *tris*(acetylacetonate) (0.018 g, 0.05 mmol), and PN (0.015 g, 0.05 mmol) are weighed neat into a 20 mL vial. THF is added (5 mL), and the reaction is stirred until homogeneous. Organomagnesium halide (1 mL @ 1 M in THF, 1 mmol) is then added in one portion, and the reaction mixture is stirred for 45 minutes (MesMgBr) or overnight (TRIPMgBr).Following this, the reaction mixture is removed from the glovebox and concentrated to dryness. The resulting residue is extracted with hexanes (3 * 2 mL) and concentrated. The crude product is then purified by silica gel chromatography using a 0.8 mmOD, 10 inch column packed with ~2 g of dry silica, eluted from pure hexanes unless otherwise specified.

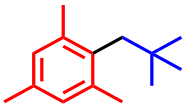

Neopentylmesitylene. ^{1}H NMR (500 MHz, Chloroform-*d*) δ 6.84 (s, 2H), 2.63 (s, 2H), 2.30 (s, 6H), 2.25 (s, 3H), 0.95 (s, 9H); ^{13}C NMR (125 MHz, Chloroform-*d*) δ 137.88, 135.26, 135.24, 128.58, 47.18, 33.16, 29.53, 20.92, 19.63. HRMS (EI^{+}) calcd for $C_{14}H_{22}$ [M]$^{+}$: 190.1721, found: 190.1722.

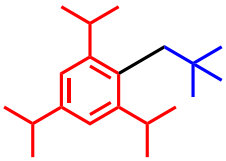

Neopentyltriisopropylbenzene. (Note: 2 equivalents of TRIPMgBr were used, 24 h reaction time) ^{1}H NMR (500 MHz, Chloroform-*d*) δ 6.97 (s, 1H), 6.92 (s, 1H), 3.35 – 3.30 (m, 1H), 2.92 – 2.82 (m, 2H), 2.71 (s, 2H), 1.26 (d, *J* = 6.8 Hz, 12H), 1.26 (d, *J* = 6.7 Hz, 6H), 0.96 (s, 9H); ^{13}C NMR (126 MHz, Chloroform-*d*) δ 148.63, 148.05, 122.03, 120.60, 37.81, 34.23, 33.88, 30.44, 29.67, 24.11, 24.01. HRMS (EI+) calcd. for $C_{20}H_{34}$ [M]$^{+}$: 274.2664, found: 274.2661.

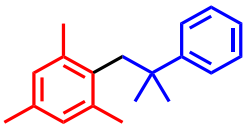

Neophylmesitylene. ^{1}H NMR (500 MHz, Chloroform-*d*) δ 7.36 – 7.26 (m, 7H), 6.95 – 6.92 (m, 2H), 2.61 (s, 6H), 2.33 (s, 3H), 1.87 (s, 6H); ^{13}C NMR (126 MHz, Chloroform-*d*) δ 136.96, 135.96, 135.47, 133.90, 133.75, 129.85, 128.26, 124.43, 120.61, 45.50, 29.69, 21.10, 19.81, 19.75. HRMS (EI^{+}) calcd for $C_{19}H_{24}$ [M]$^{+}$: 252.1886, found: 252.1878.

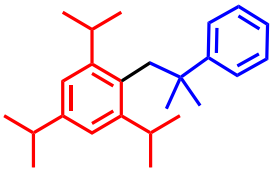

Neophyltriisopropylbenzene. (Note: 2 equivalents of TRIPMgBr were used, 24 h reaction time) ^{1}H NMR (500 MHz, Chloroform-*d*) δ 7.36 – 7.27 (m, 5H), 6.96 (d, *J* = 1.6 Hz, 2H), 3.13 – 3.00 (m, 4H), 2.95 – 2.82 (m, 1H), 1.38 (d, *J* = 1.6 Hz, 6H), 1.32 – 1.24 (m, 6H), 1.14 – 1.03 (m, 12H); ^{13}C NMR (126 MHz, Chloroform-*d*) δ 150.63, 148.27, 146.23, 129.83, 127.89, 126.01, 125.53, 120.48, 39.63, 39.29, 33.97, 29.90, 29.84, 29.04, 28.99, 24.05, 24.02. HRMS (EI^{+}) calcd for $C_{25}H_{36}$ [M]$^{+}$: 336.2822, found: 336.2817.

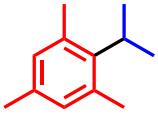

Isopropylmesitylene. ^{1}H NMR (500 MHz, Chloroform-*d*) δ 6.58 (d, *J* = 1.8 Hz, 2H), 3.26 (p, J = 6.4 Hz, 1H), 2.30 (d, J = 0.9 Hz, 6H), 2.21 – 2.04 (m, 3H), 1.28 (d, *J* = 6.4 Hz, 6H); ^{13}C NMR (125 MHz, Chloroform-*d*) δ 142.86, 137.04, 135.33, 129.22, 31.80, 22.04, 20.92, 19.54. HRMS (EI^{+}) calcd for $C_{12}H_{18}$ [M]$^{+}$: 162.1408, found: 162.1409.

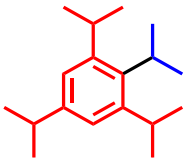

1,2,3,5-tetraisopropylbenzene. (Note: 2 equivalents of TRIPMgBr were used, 24 h reaction time) ^{1}H NMR (500 MHz, Chloroform-*d*) δ 7.01 (s, 2H), 2.94 (q, *J* = 6.9 Hz, 2H), 2.45 (p, *J* = 6.7 Hz, 2H), 1.31 (dd, J = 7.1, 2.1 Hz, 12H), 1.08 (d, J = 6.7 Hz, 12H); ^{13}C NMR (126 MHz, Chloroform-

d) δ 147.69, 147.14, 133.23, 120.99, 120.93, 34.07, 29.61, 25.36, 24.23, 24.18. HRMS (EI$^+$) calcd for $C_{18}H_{30}$ [M]$^+$: 246.2347, found: 246.2339.

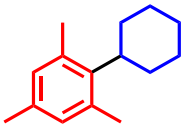

Cyclohexylmesitylene. ^{1}H NMR (500 MHz, Chloroform-*d*) δ 6.58 (d, J = 1.6 Hz, 2H), 2.81 (ddd, *J* = 7.4, 5.1, 2.2 Hz, 1H), 2.24 (s, 6H), 2.13 (d, *J* = 1.0 Hz, 3H), 1.88 (ddd, *J* = 10.0, 5.9, 4.2 Hz, 6H), 1.85 – 1.64 (m, 4H); ^{13}C NMR (125 MHz, Chloroform-*d*) δ 138.99, 138.17, 135.89, 128.77, 39.36, 31.00, 25.52, 24.56, 20.92, 19.54. HRMS (EI$^+$) calcd for $C_{15}H_{22}$ [M]$^+$: 202.1721, found: 202.1720.

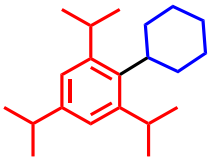

Cyclohexyltriisopropylbenzene. (Note: 2 equivalents of TRIPMgBr were used, 24 h reaction time) ^{1}H NMR (500 MHz, Chloroform-*d*) δ 6.98 (s, 2H), 3.19 (m, 2H), 2.95 – 2.80 (m, 2H), 1.95 – 1.70 (m, 10H), 1.20 (m, 18H); ^{13}C NMR (125 MHz, Chloroform-*d*) δ 151.91, 149.43, 141.87, 123.66, 36.50, 34.37, 30.99, 30.06, 25.52, 24.56, 23.82, 23.42. HRMS (EI$^+$) calcd for $C_{21}H_{34}$ [M]$^+$: 286.2660, found: 286.2661.

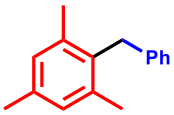

Benzylmesitylene. ^{1}H NMR (500 MHz, Chloroform-*d*) δ 7.32 – 7.16 (m, 3H), 7.04 (d, *J* = 7.6 Hz, 2H), 6.92 (s, 2H), 4.05 (s, 2H), 2.33 (s, 3H), 2.24 (s, 6H); ^{13}C NMR (125 MHz, Chloroform-*d*) δ 139.65, 137.00, 135.63, 128.89, 128.81, 127.81, 125.62, 34.69, 20.92, 20.09. HRMS (EI^{+}) calcd for $C_{16}H_{18}$ [M]$^{+}$: 210.1409, found: 210.1409.

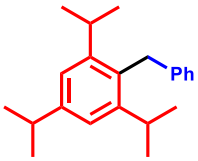

Benzyltriisopropylbenzene. (Note: 2 equivalents of TRIPMgBr were used, 24 h reaction time) ^{1}H NMR (500 MHz, Chloroform-*d*) δ 7.34 – 7.23 (m, 2H), 7.22 – 7.14 (m, 2H), 7.07 (m, 3H), 4.16 (s, 2H), 3.14 – 3.03 (m, 2H), 2.95 (m, 1H), 1.40 – 1.26 (m, 6H), 1.22 – 1.13 (m, 12H); ^{13}C NMR (126 MHz, Chloroform-*d*) δ 147.36, 146.93, 141.47, 130.66, 128.19, 127.90, 125.53, 120.98, 34.14, 32.99, 29.59, 24.17, 24.09. HRMS (EI^{+}) calcd for $C_{22}H_{30}$ [M]$^{+}$: 294.2346, found: 296.2348.

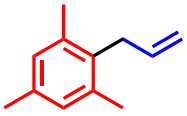

3-(2,4,6-trimethyl)phenylpropene. ^{1}H NMR (500 MHz, Chloroform-*d*) δ 6.92 (s, 2H), 5.99 – 5.92 (m, 1H), 5.05 (m, 1H), 4.94 (m, 1H), 3.43 (d, *J* = 5.5 Hz, 2H), 2.33 (s, 9H); ^{13}C NMR (125 MHz, Chloroform-*d*) δ 136.64, 135.63, 135.48, 133.14, 128.90, 128.32, 114.79, 33.46, 20.97. HRMS (EI^{+}) calcd for $C_{12}H_{16}$ [M]$^{+}$: 160.1252, found: 160.1252.

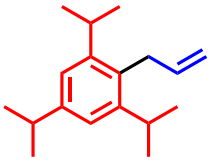

3-(2,4,6-triisopropyl)phenylpropene.. ^{1}H NMR (500 MHz, Chloroform-*d*) δ 7.00 (s, 2H), 6.02 – 5.95 (m, 1H), 5.00 (dd, *J* = 10.5, 2.5 Hz, 1H), 4.87 – 4.83 (dd, *J* = 17.5, 2 Hz, 1H), 3.45 (d, *J* = 5.5 Hz, 2H), 3.13 (sept, *J* = 7 Hz, 2H), 2.88 (m, 1H), 1.26 (d, *J* = 7 Hz, 12H) 1.22 (d, *J* = 7 Hz, 6H); ^{13}C NMR (125 MHz, Chloroform-*d*) δ 147.13, 138.04, 122.20, 121.00, 115.05, 34.40, 31.67, 29.43, 24.28. HRMS (EI^{+}) calcd for $C_{18}H_{28}$ [M]$^{+}$: 244.2191, found: 244.2193

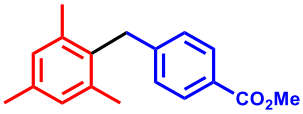

Methyl 4-(2,4,6-trimethylbenzyl)benzoate. ^{1}H NMR (500 MHz, Chloroform-*d*) δ 7.98 – 7.87 (m, 2H), 7.33 (m, 2H), 6.64 (m, 2H), 4.03 (s, 2H), 3.91 (s, 3H), 2.31 (s, 6H), 2.20 – 2.01 (m, 3H); ^{13}C NMR (125 MHz, Chloroform-*d*) δ 168.55, 142.74, 137.26, 137.20, 135.53, 128.79, 128.64, 127.89, 124.99, 52.37, 37.85, 20.92, 19.63. HRMS (EI^{+}) calcd for $C_{18}H_{20}O_2$ [M]$^{+}$: 268.1463, found: 268.1463.

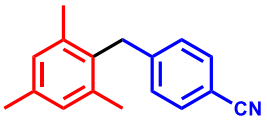

4-(2,4,6-trimethylbenzyl)benzonitrile. ^{1}H NMR (500 MHz, Chloroform-*d*) δ 7.52 (d, *J* = 8.5 Hz, 2H), 7.11 (d, *J* = 8.5 Hz, 2H), 6.91 (s, 2H), 4.06 (s, 2H), 2.30 (s, 3H), 2.17 (s, 6H); ^{13}C NMR (125 MHz, Chloroform-*d*) δ 146.22, 137.02, 136.52, 132.36, 129.26, 128.73, 124.95, 119.25, 109.78, 35.04, 21.06, 20.24. HRMS (EI^{+}) calcd for $C_{17}H_{17}N$ [M]$^{+}$: 235.1361, found: 235.1356.

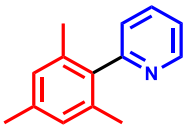

2-(2,4,6-trimethylbenzyl)pyridine. ^{1}H NMR (500 MHz, Chloroform-*d*) δ 8.73 (m, 1H), 7.76 (td, *J* = 7.5, 2 Hz, 1H), 7.28-7.23 (m, 2H), 6.95 (s, 2H), 2.34 (s, 3H), 2.03 (s, 6H); ^{13}C NMR (125 MHz, Chloroform-*d*) δ 160.30, 149.89, 137.60, 136.38, 135.87, 128.49, 124.92, 121.73, 21.35, 20.36. HRMS (EI^{+}) calcd for $C_{14}H_{15}N$ [M]$^{+}$: 197.1205, found: 197.1207.

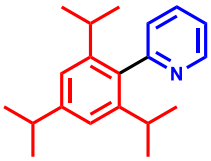

2-(2,4,6-triisopropylbenzyl)pyridine. ^{1}H NMR (500 MHz, Chloroform-*d*) δ 8.69-8.67 (dq, *J* = 5, 1 Hz, 1H), 7.72-7.69 (td, *J* = 8, 2 Hz, 1H), 7.28 (m, 1H), 7.05 (s, 2H), 6.90 (d, *J* = 2.5 Hz, 1H) 2.92 (sept, *J* = 7 Hz, 1H), 2.47 (sept, *J* = 6.5 Hz, 2H), ; ^{13}C NMR (125 MHz, Chloroform-*d*) δ 171.28, 149.41, 146.29, 135.72, 125.20, 121.54, 120.76, 34.57, 30.46, 24.41, 24.25, 24.03, 22.81. HRMS (EI^{+}) calcd for $C_{20}H_{27}N$ [M]$^{+}$: 218.2143, found: 218.2144.

2.6.4 Tolerance Screen

General Procedure. To a 1 mL solution of benzyl bromide (0.1 mmol, 17.1 mg, 0.1 M) in THF was added a solution of $Co(acac)_3$ (0.01 mmol, 3.6 mg, 0.01 M), PN (0.02 mmol, 6.11 mg, 0.02 M), and *tert*-butylbenzene (0.1 mmol, 13.4 mg, 0.1 M) in 1 mL THF followed by a 1 mL THF solution of additive (0.1 mmol, 0.1 M). A 0.1 mL solution of mesitylmagnesium bromide (0.1 mmol, 22.3 mg, 1.0 M) in THF was added dropwise to the mixture while stirring. The solution was allowed to stir at room temperature for three hours. An aliquot was taken 30 min after

addition of organomagnesium for analysis by GC-MS, followed by another aliquot each hour after the start of the reaction for three hours.

Table 2.5: Tolerance Screen Results.

Additive	Time (min)	Additive Remaining	error	Product %	error
Benzonitrile	30	19 %	1 %	77 %	6 %
	60	24 %	4 %	77 %	1 %
	90	22 %	3 %	80 %	3 %
	120	24 %	6 %	79 %	4 %
Me_2NPh	30	50 %	3 %	54 %	4 %
	60	50 %	3 %	54 %	2 %
	90	75 %	4 %	55 %	4 %
	120	76 %	3 %	56 %	3 %
OctOH	30	47 %	5 %	3 %	1 %
	60	48 %	4 %	3 %	1 %
	90	44 %	8 %	3 %	1 %
	120	50 %	3 %	4 %	1 %
1-Decyne	30	24 %	8 %	27 %	4 %
	60	24 %	7 %	23 %	5 %
	90	25 %	8 %	30 %	4 %
	120	26 %	6 %	31 %	4 %
$PhCO_2Me$	30	90 %	2 %	91 %	2 %
	60	91 %	2 %	92 %	1 %
	90	91 %	2 %	91 %	1 %
	120	91 %	1 %	92 %	1 %

Table 2.5 (cont.)

N-methyl-*N*-phenylacetamide	30	93 %	3 %	56 %	3 %
	60	93 %	1 %	70 %	6 %
	90	96 %	3 %	69 %	7 %
	120	94 %	4 %	68 %	7 %
acetophenone	30	78 %	1 %	35 %	4 %
	60	77 %	1 %	35 %	3 %
	90	79 %	2 %	35 %	3 %
	120	77 %	4 %	34 %	1 %
3,5-lutidine	30	32 %	1 %	92 %	4 %
	60	29 %	2 %	96 %	1 %
	90	30 %	3 %	97 %	1 %
	120	29 %	3 %	97 %	2 %
limonene	30	95 %	2 %	54 %	3 %
	60	95 %	5 %	55 %	5 %
	90	93 %	2 %	56 %	4 %
	120	96%	2 %	56 %	4 %
Control	30	--	--	95 %	2 %
	60	--	--	97 %	2 %
	90	--	--	97 %	1 %
	120	--	--	97 %	1 %

2.6.5 Synthesis of (PN)CoMes$_2$

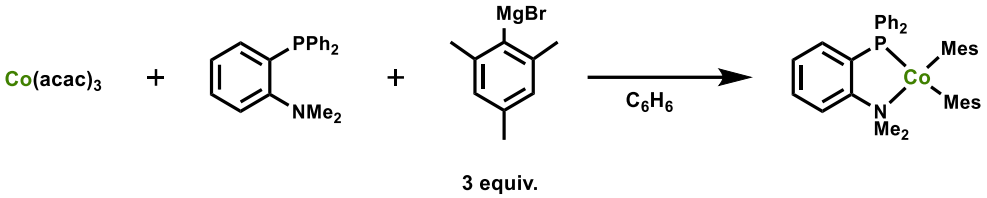

A 20 mL scintillation vial was charged with Co(acac)$_3$ (89.1 mg, 0.25 mmol) and PN (76.3 mg, 0.25 mmol). 2 mL benzene was added, and the dark green solution was placed in a freezer until frozen. The vial was allowed to slowly thaw while stirring, after which MesMgBr (1.0 M in THF, 0.75 mL, 0.75 mmol) was added dropwise, resulting in rapid color change to a dark orange solution. The mixture was frozen once again and solvent lyophilized to yield a dark orange solid. The solid was dissolved in 3 mL toluene, filtered over a pad of Celite®, and concentrated to incipient solid formation. Allowing the concentrated solution to cool to -35°C overnight yielded bright orange crystals (108.5 mg, 72%). ^{1}H NMR (500 MHz, C_6D_6) δ 26.03, 14.23, 9.16, 8.98, 7.98, 7.41, 6.91, 6.72, 6.58, 2.50, 2.22, 2.16, 1.93, -8.89, -22.32.

2.6.6 NMR Spectra of Substrates

Neopentylmesitylene.

^{1}H NMR – $CDCl_3$

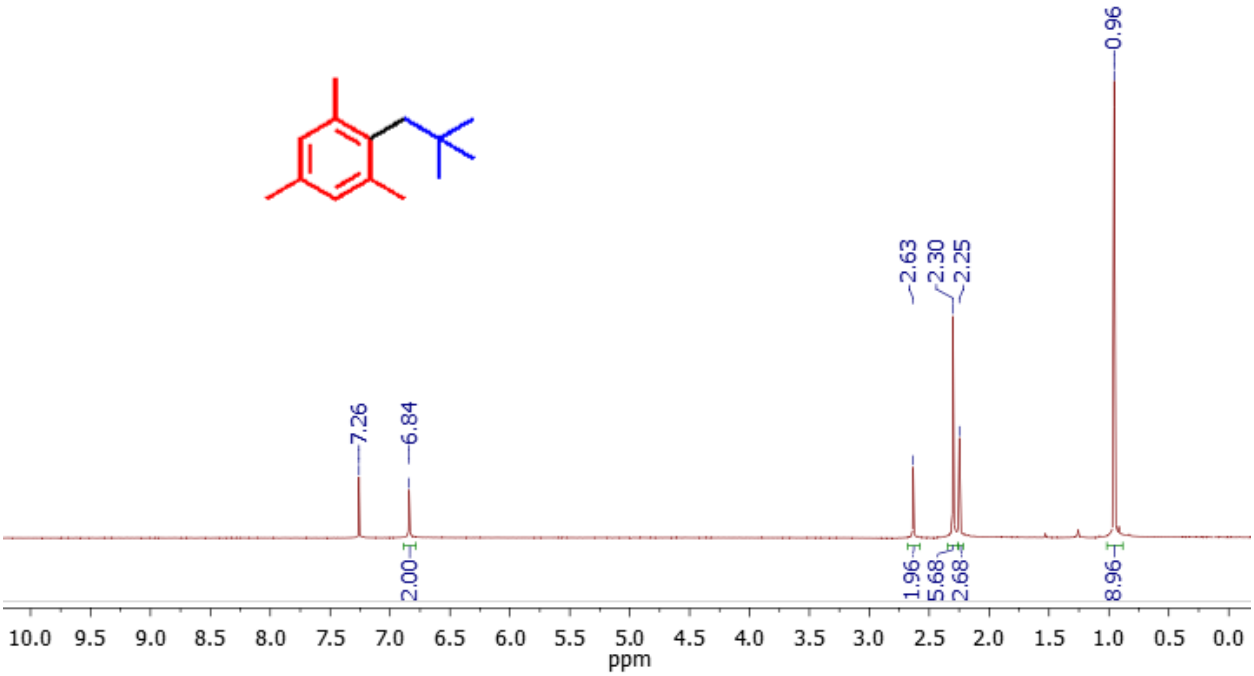

^{13}C – $CDCl_3$

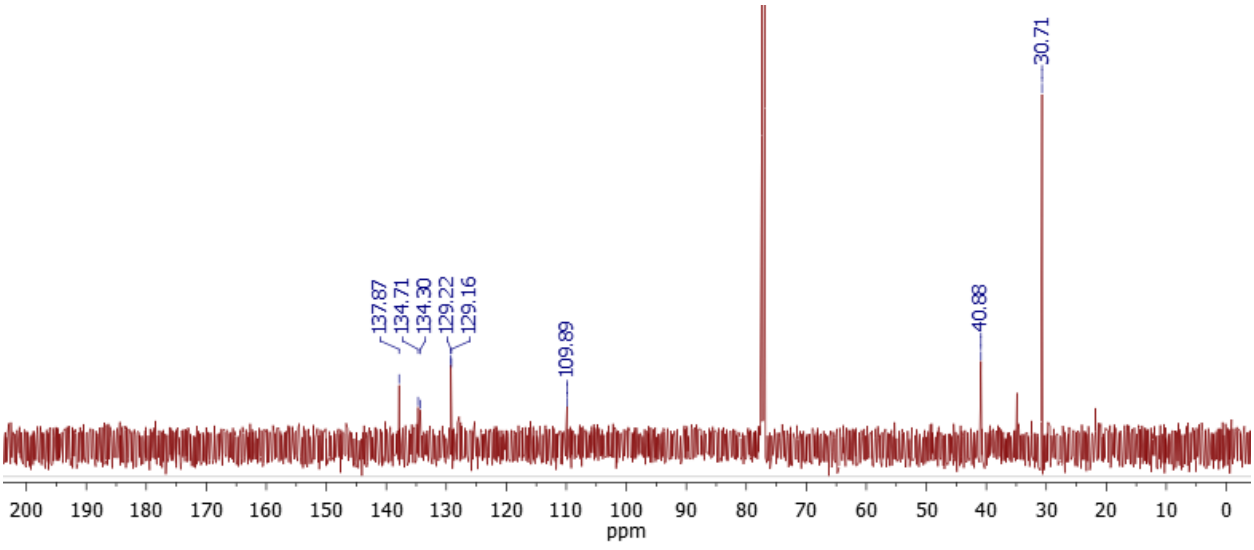

Neopentyltriisopropylbenzene.

^{1}H NMR – $CDCl_3$

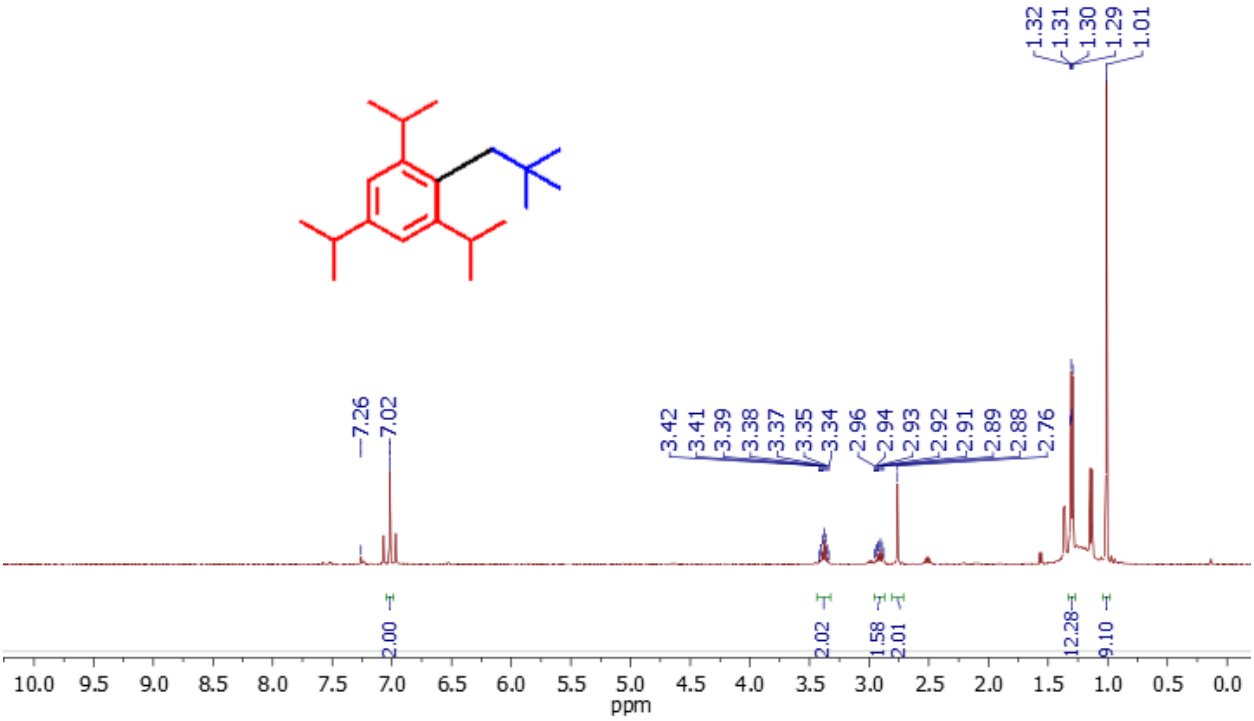

^{13}C – $CDCl_3$

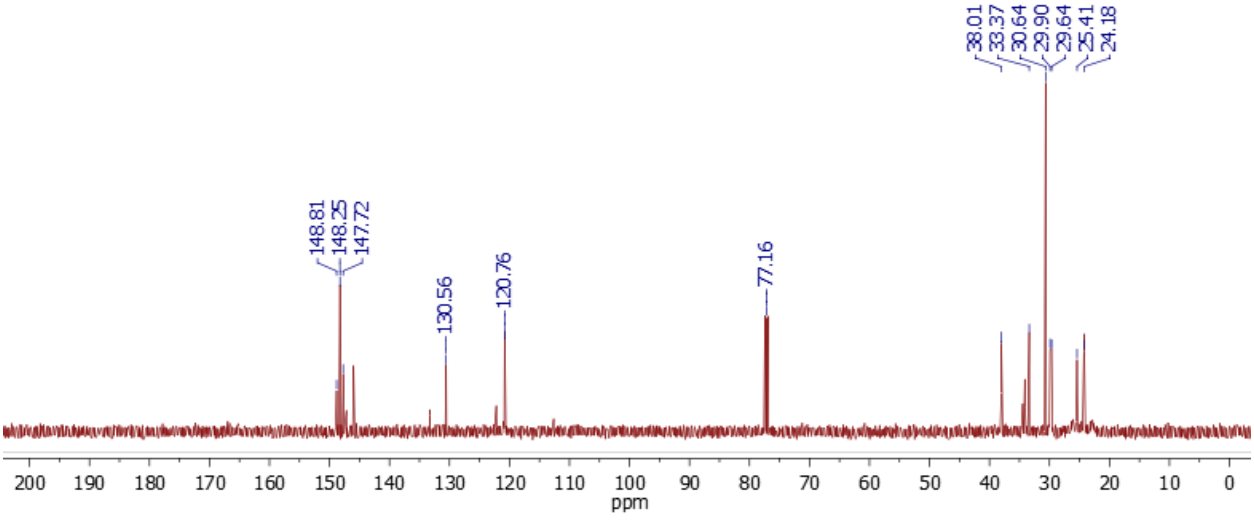

Neophylmesitylene.

^{1}H NMR – $CDCl_3$

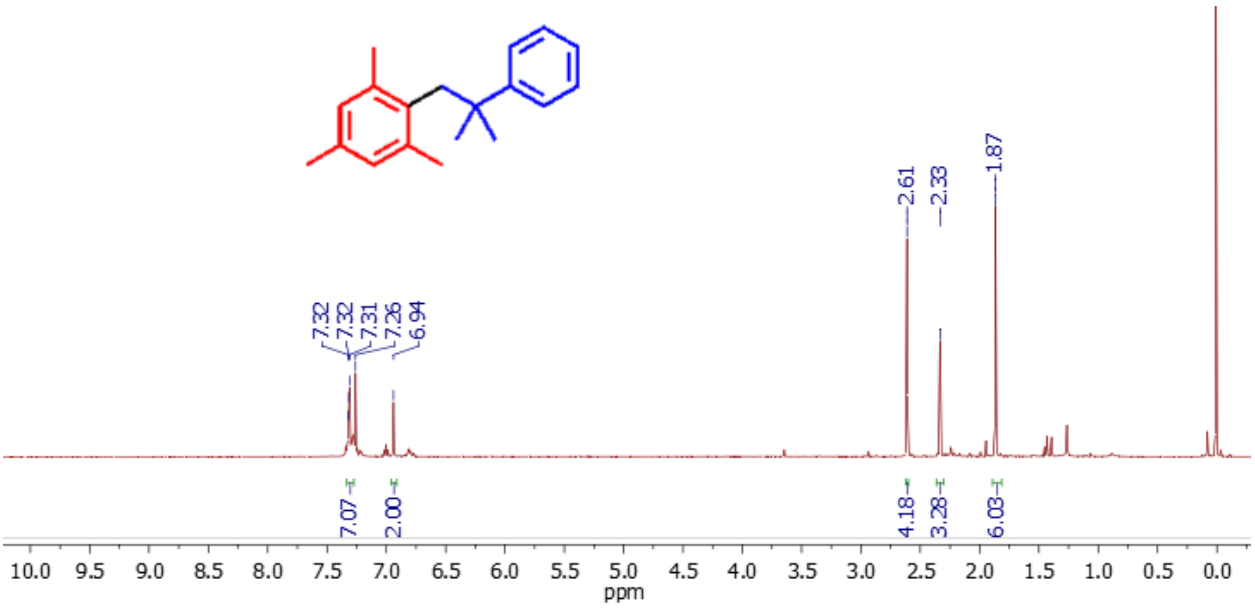

^{13}C – $CDCl_3$

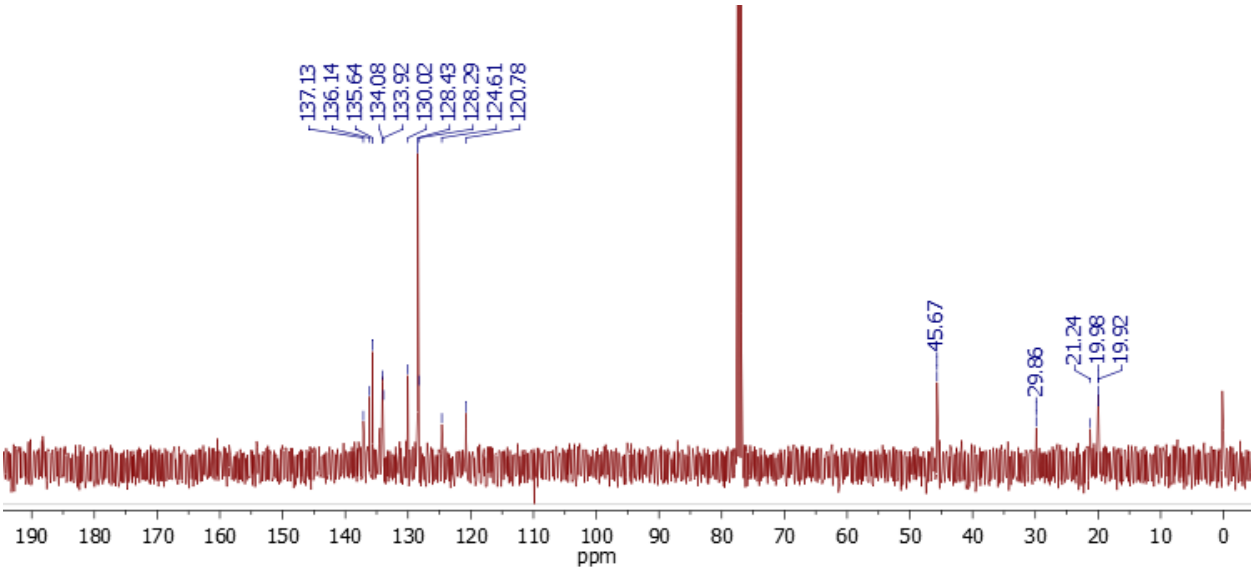

Neophyltriisopropylbenzene.

^{1}H NMR – $CDCl_3$

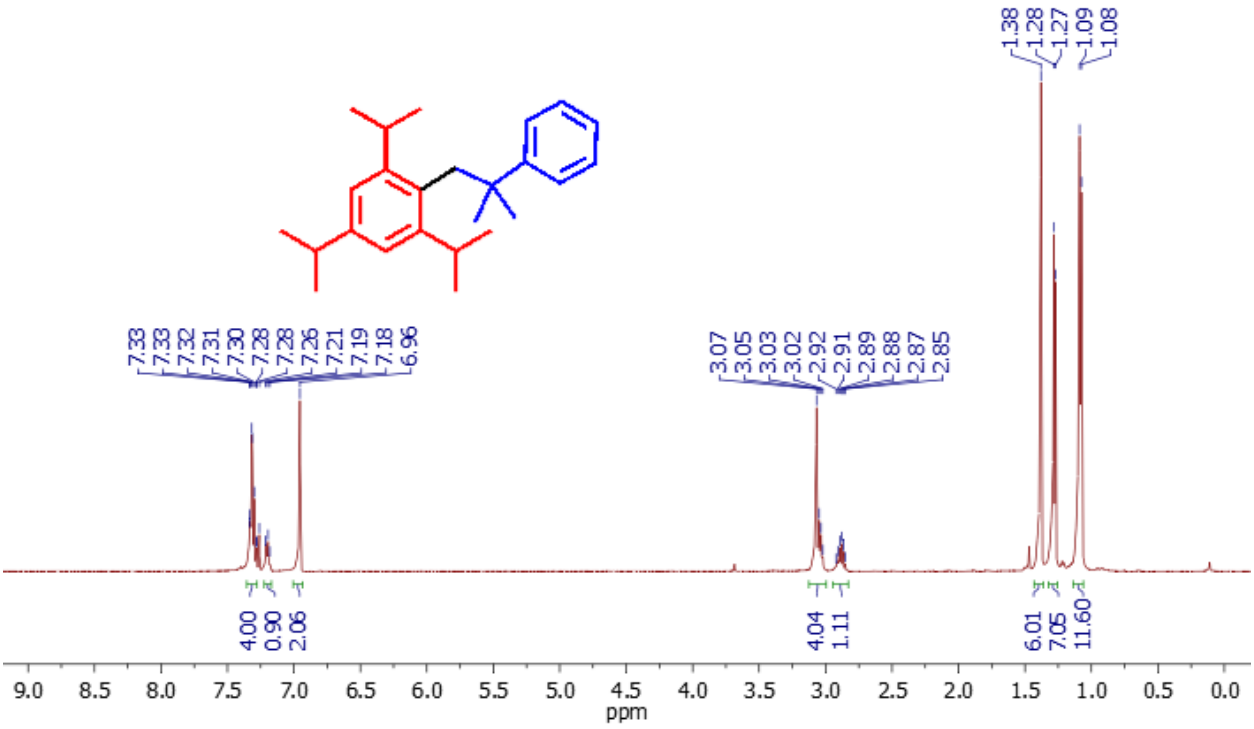

^{13}C – $CDCl_3$

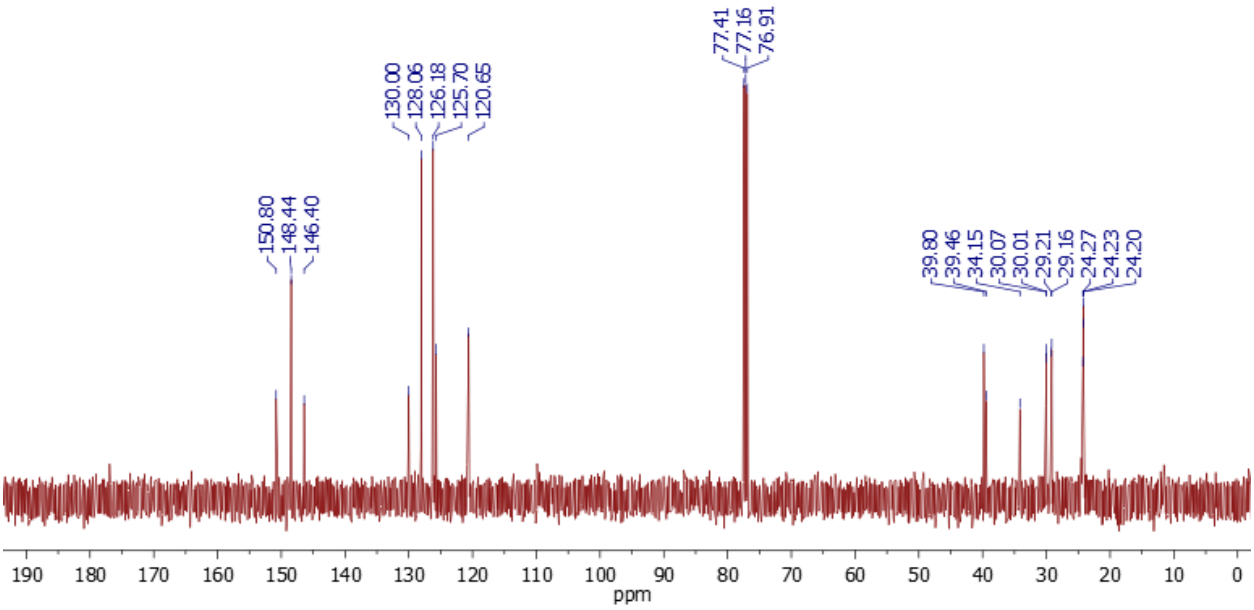

Isopropylmesitylene.

^{1}H NMR – $CDCl_3$

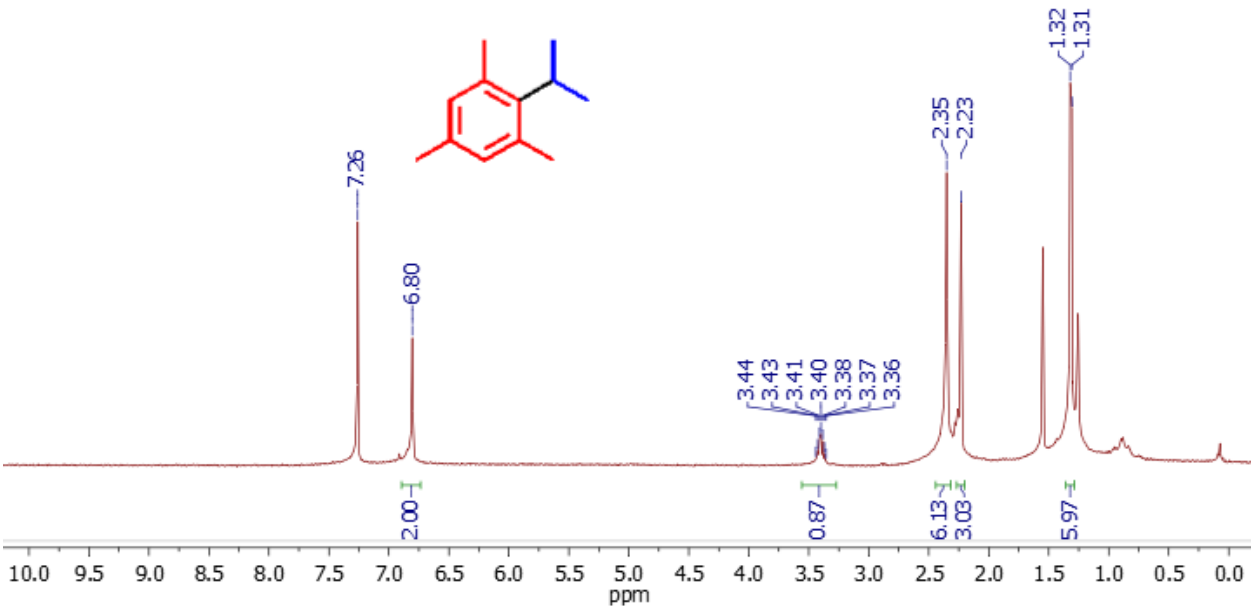

^{13}C – $CDCl_3$

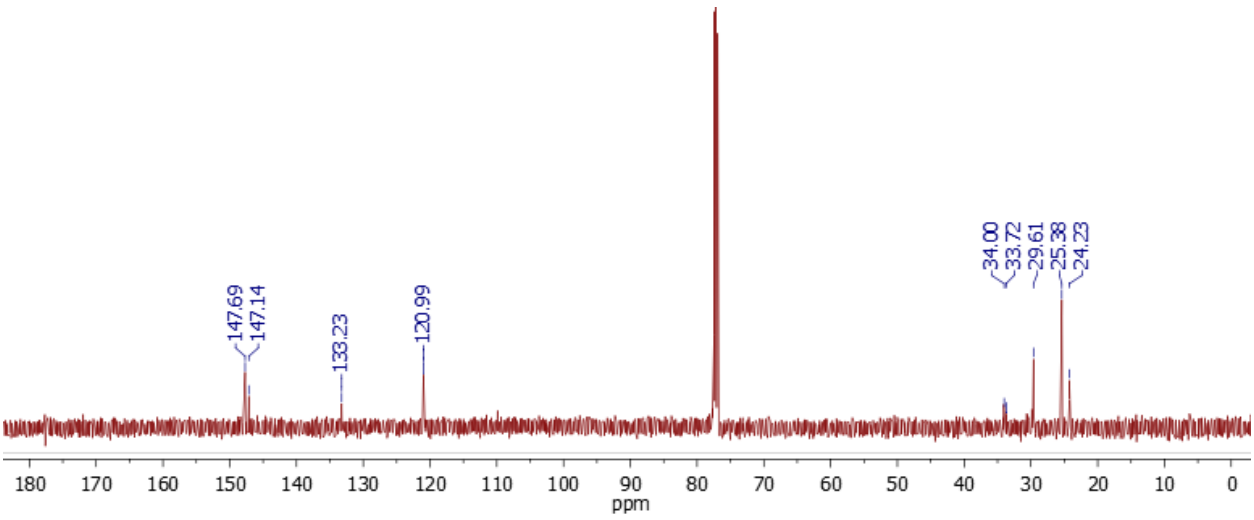

1,2,3,5-tetraisopropylbenzene.

^{1}H NMR – $CDCl_3$

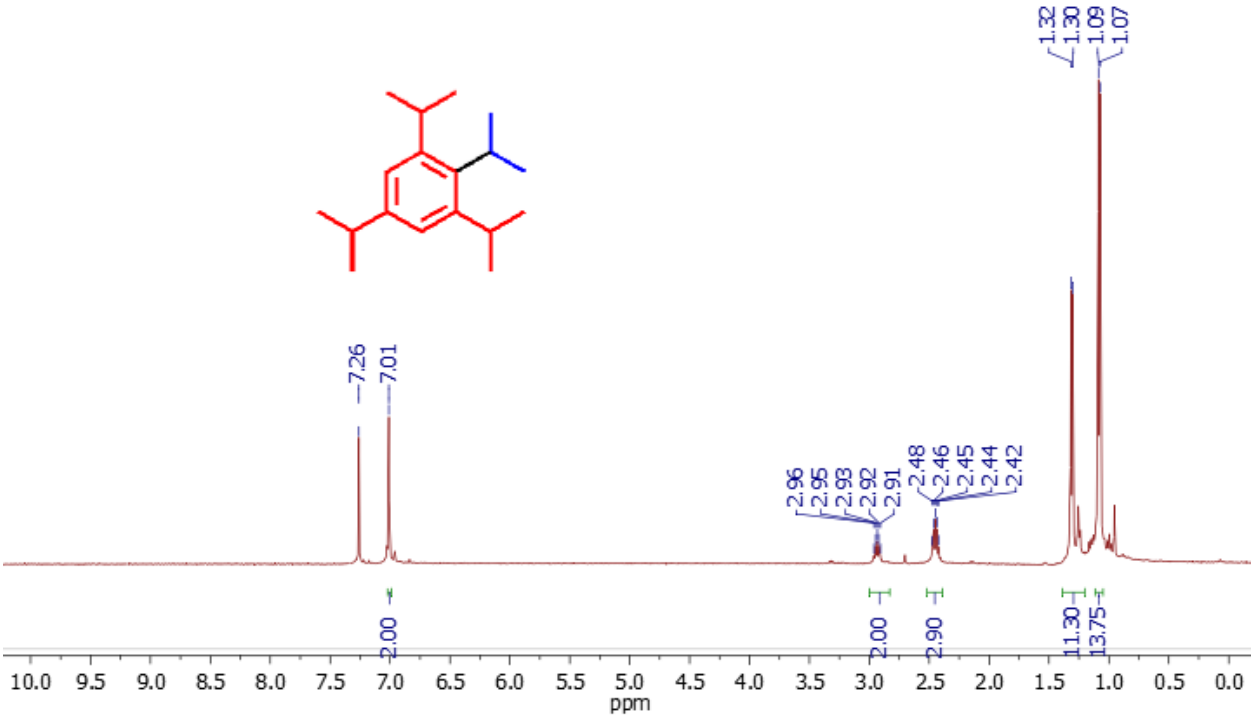

^{13}C – $CDCl_3$

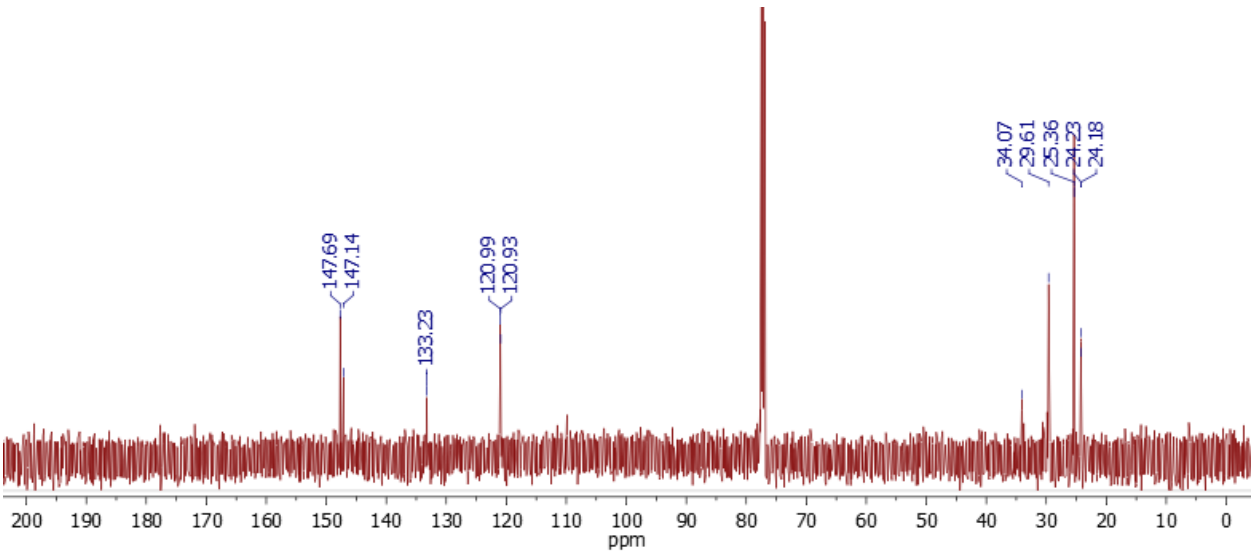

Cyclohexylmesitylene.

^{1}H NMR – $CDCl_3$

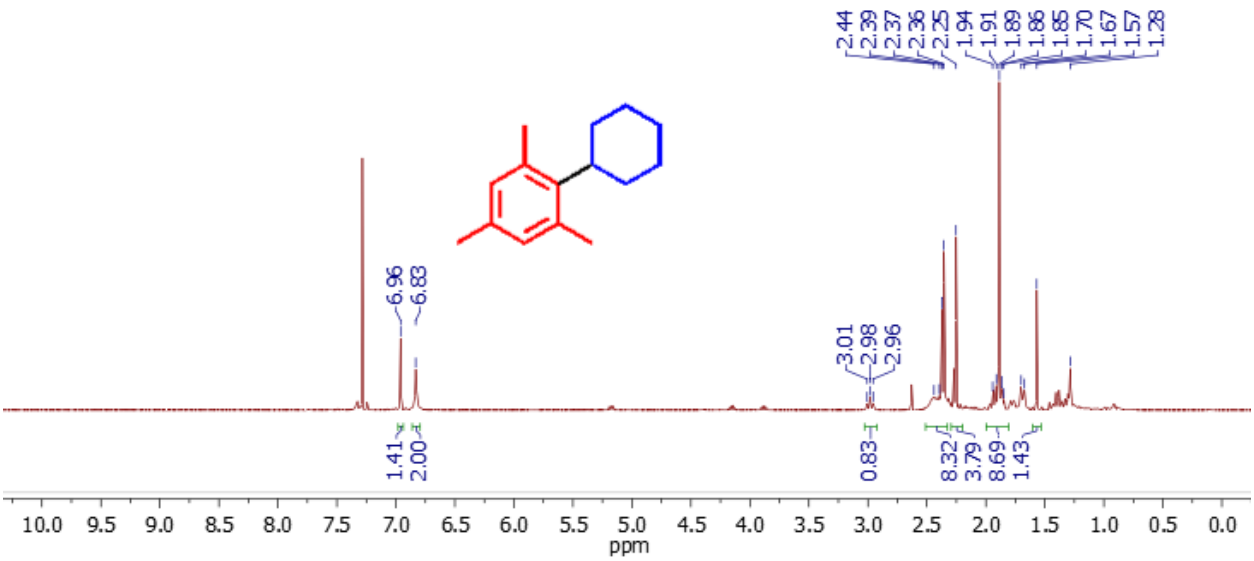

^{13}C – $CDCl_3$

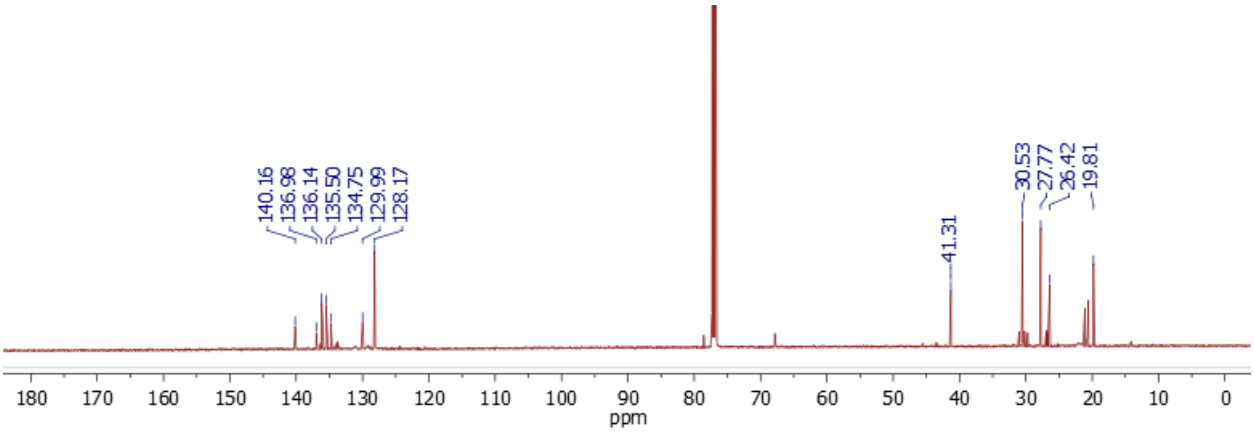

Benzylmesitylene.

^{1}H NMR – $CDCl_3$

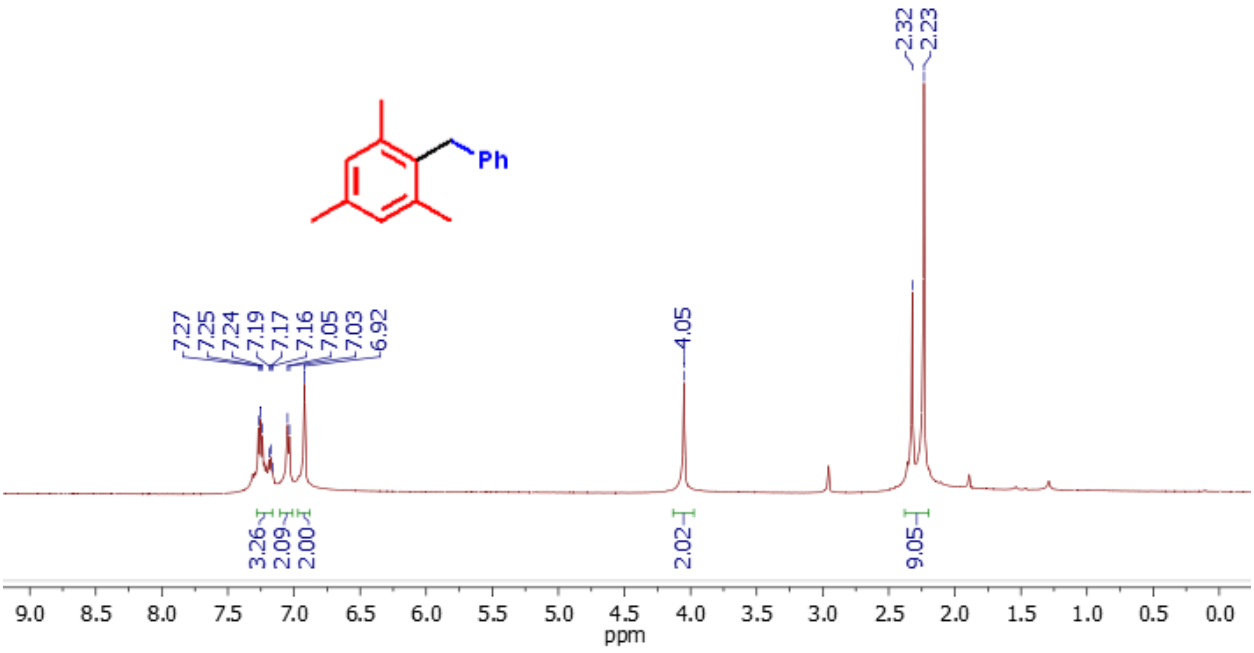

^{13}C – $CDCl_3$

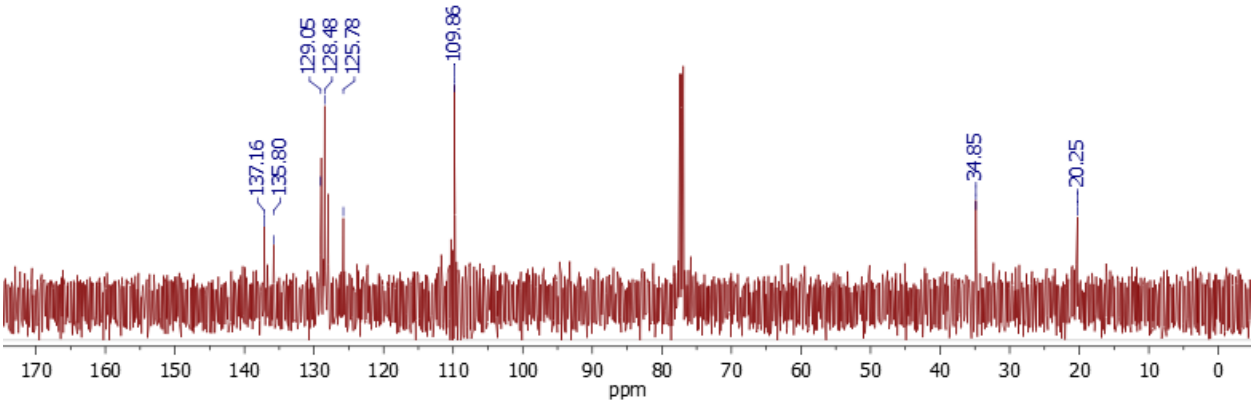

Benzyltriisopropylbenzene.

^{1}H NMR – $CDCl_3$

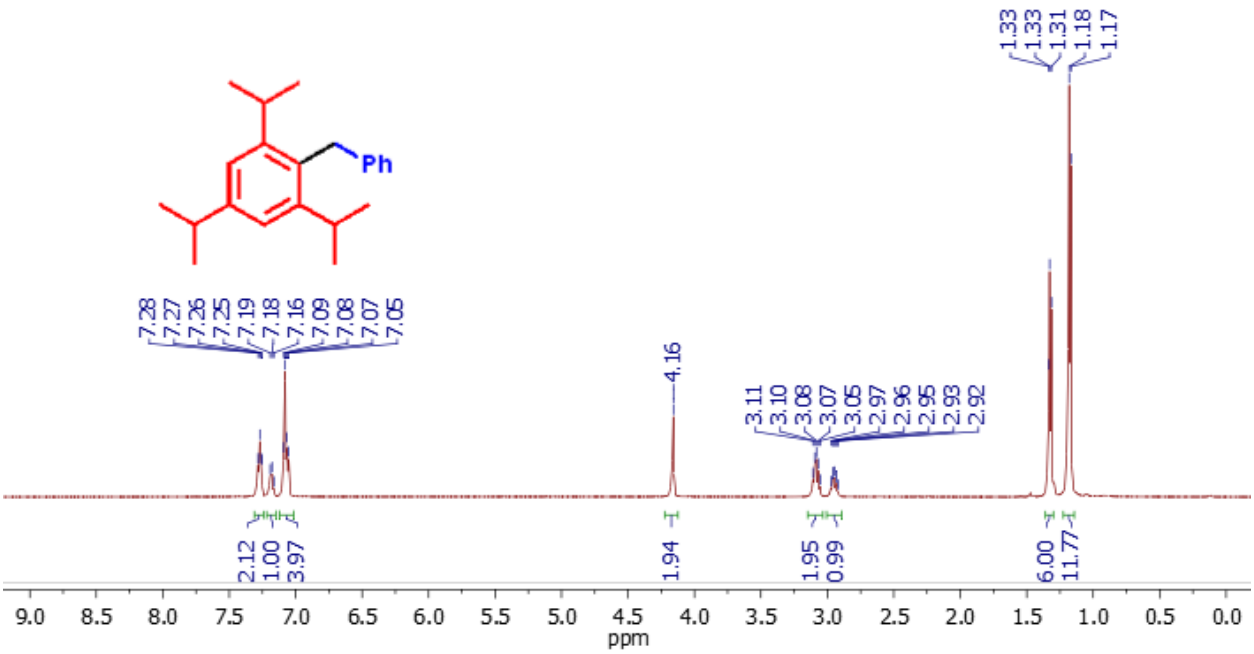

^{13}C – $CDCl_3$

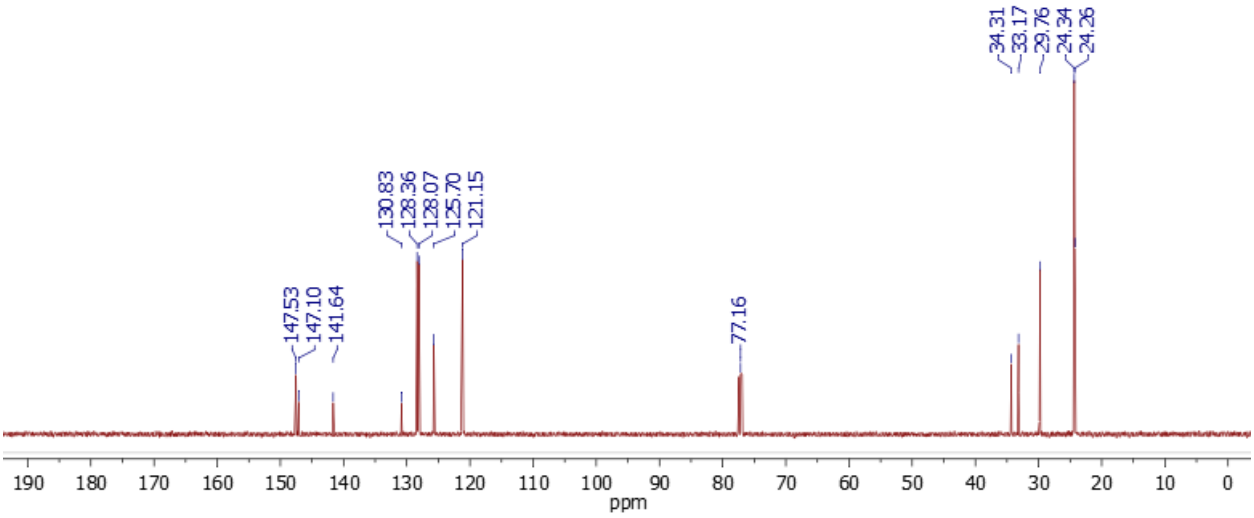

3-(2,4,6-trimethyl)phenylpropene.

^{1}H NMR – $CDCl_3$

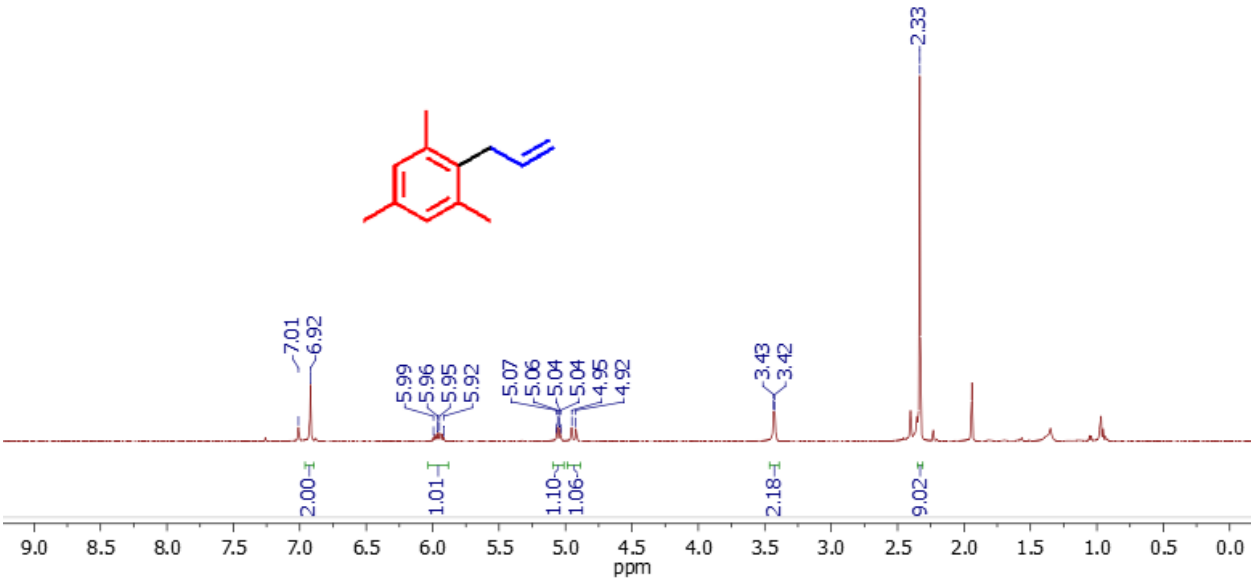

^{13}C – $CDCl_3$

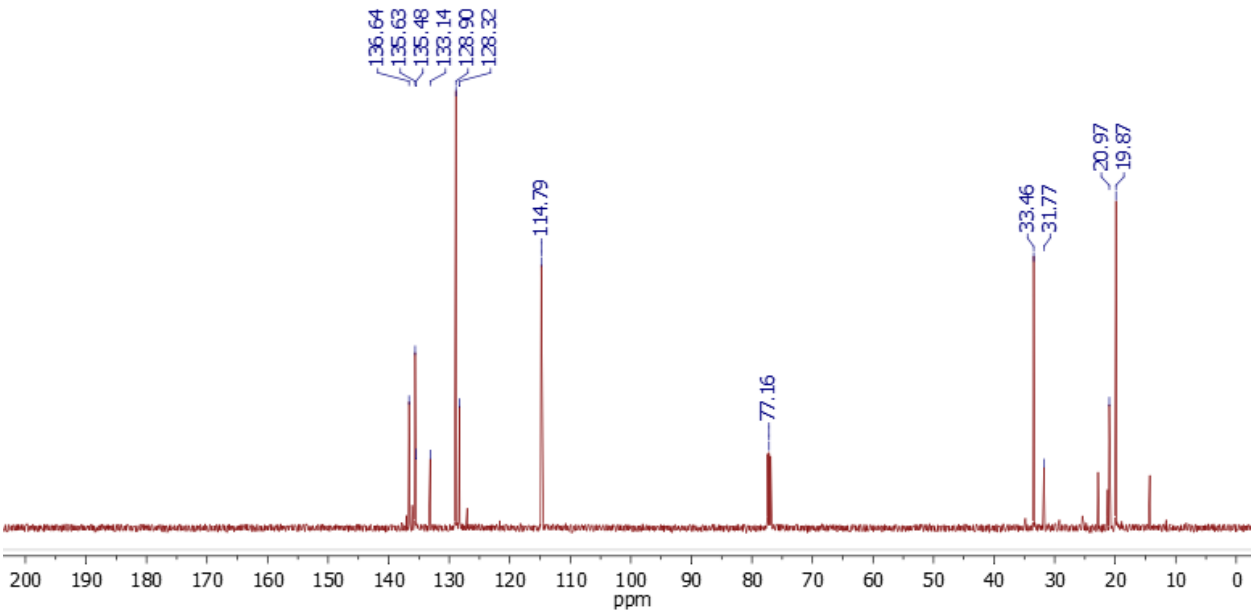

3-(2,4,6-triisopropylphenyl)propene.

^{1}H NMR – $CDCl_3$

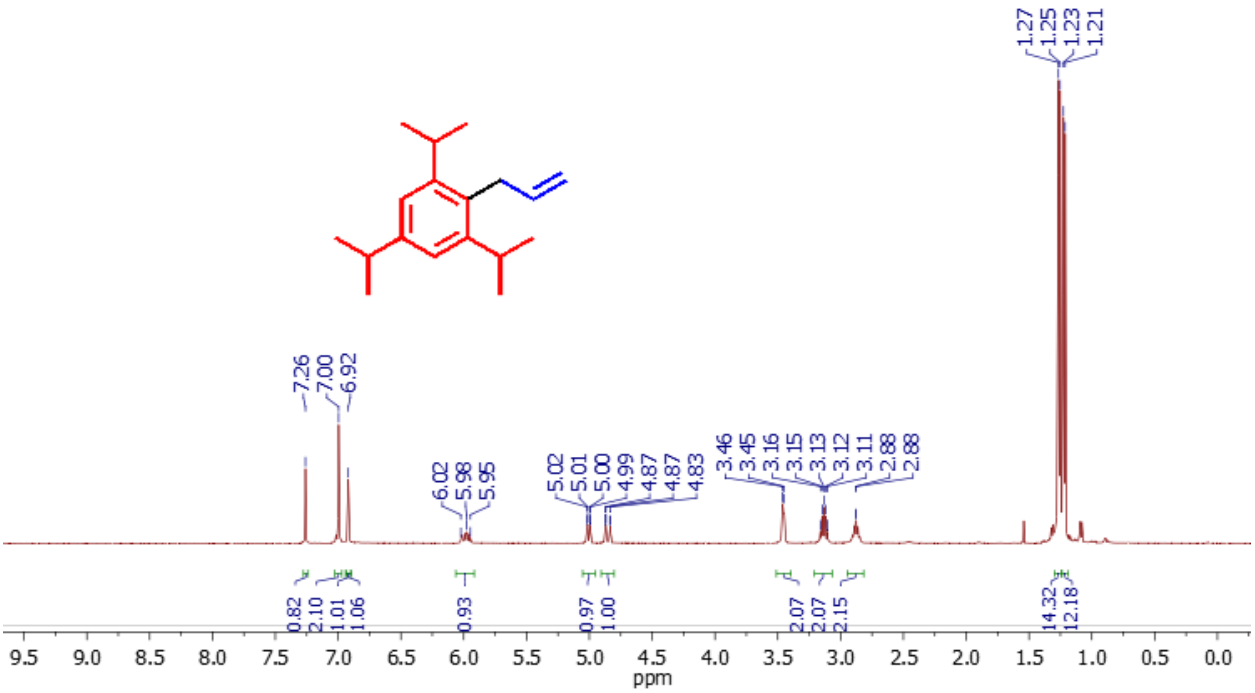

^{13}C – $CDCl_3$

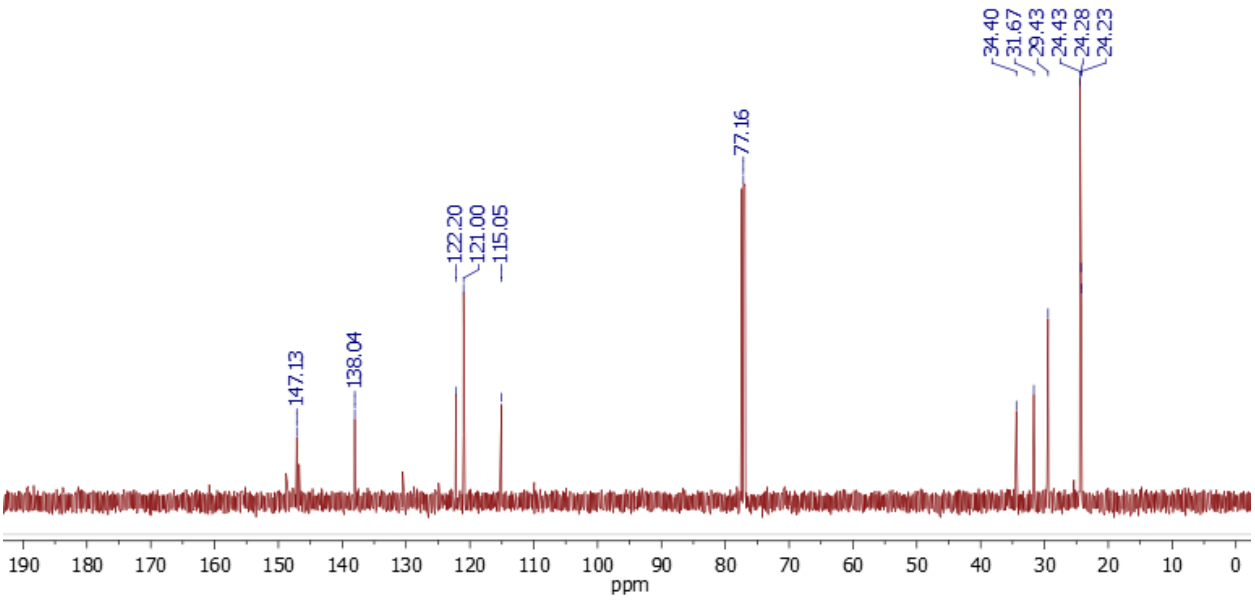

Methyl 4-(2,4,6-trimethylbenzyl)benzoate.

^{1}H NMR – $CDCl_3$

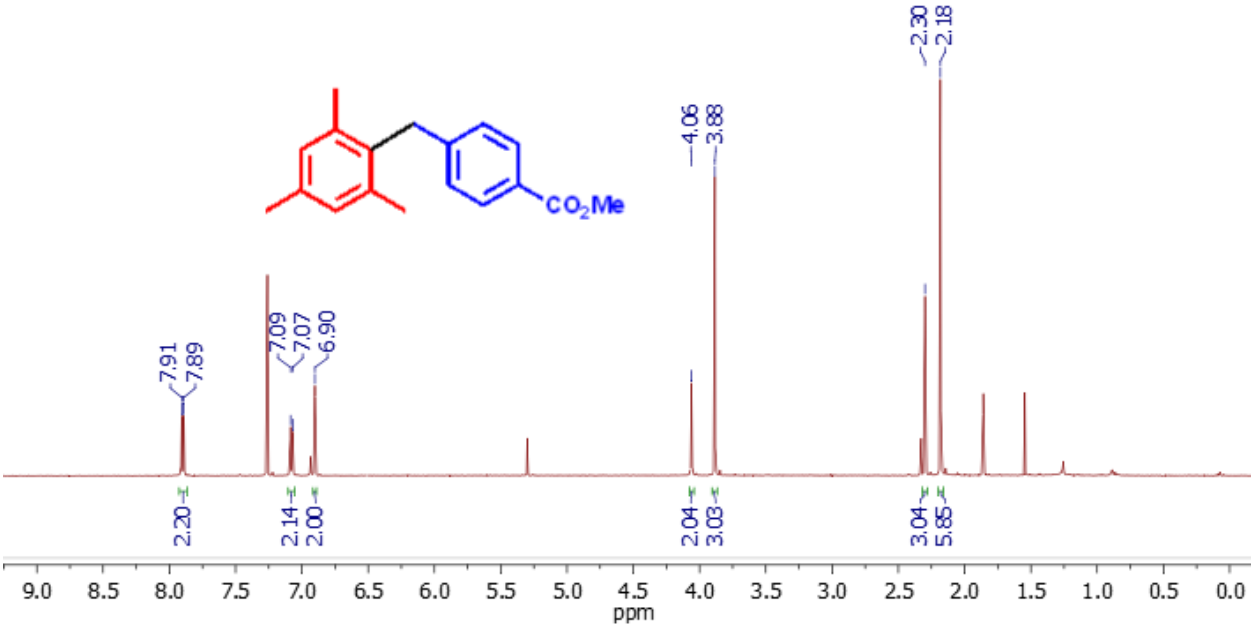

^{13}C – $CDCl_3$

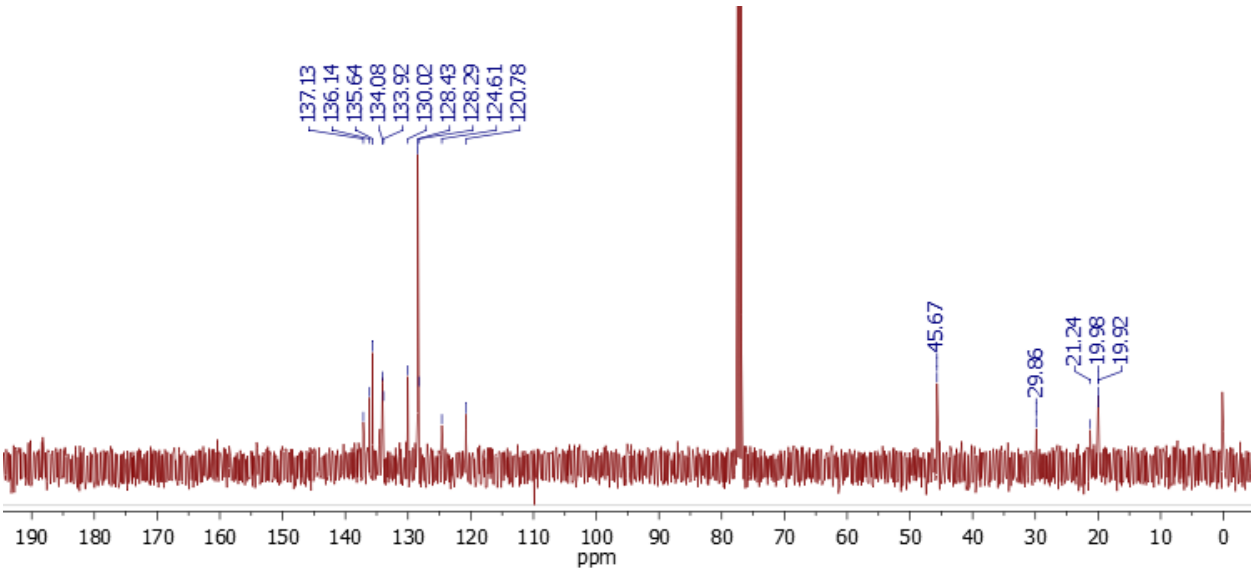

4-(2,4,6-trimethylbenzyl)benzonitrile.

^{1}H NMR – $CDCl_3$

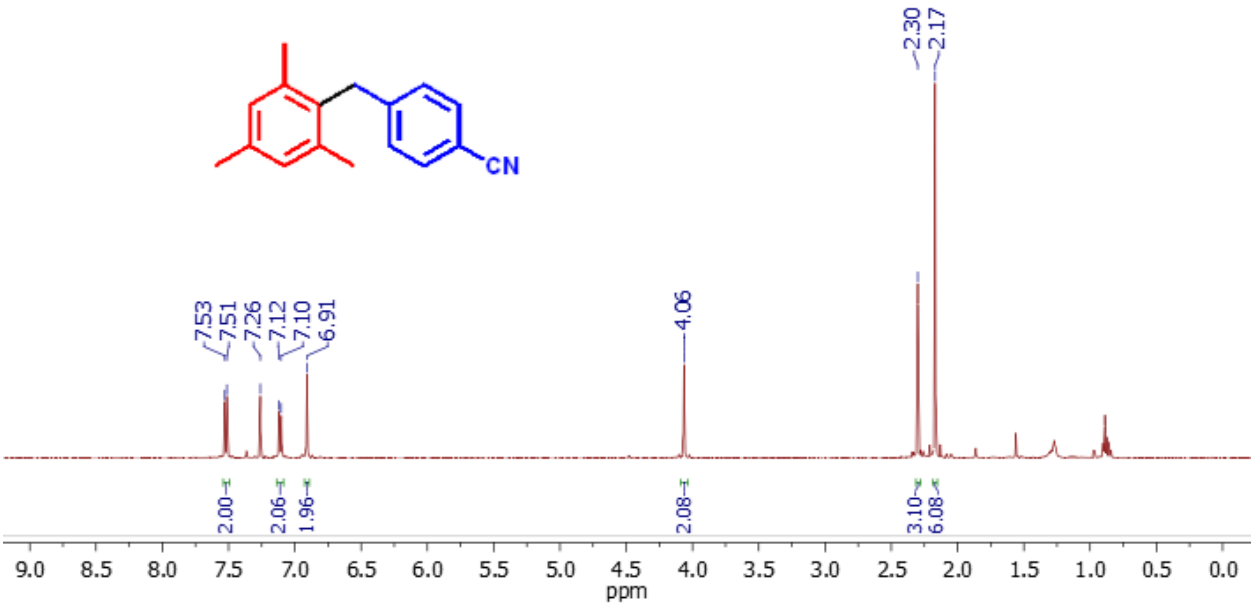

^{13}C – $CDCl_3$

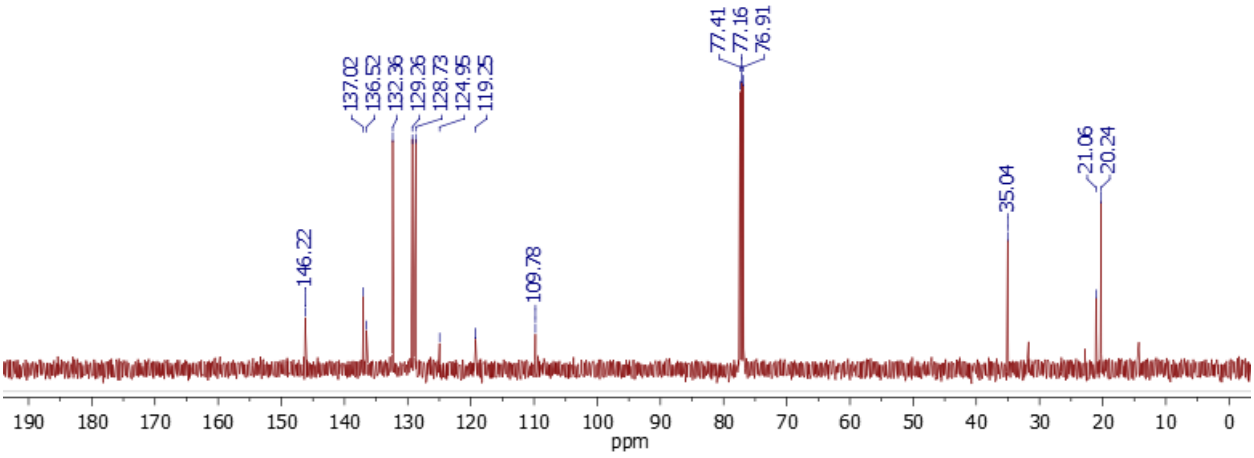

2-(2,4,6-trimethylbenzyl)pyridine.

^{1}H NMR – $CDCl_3$

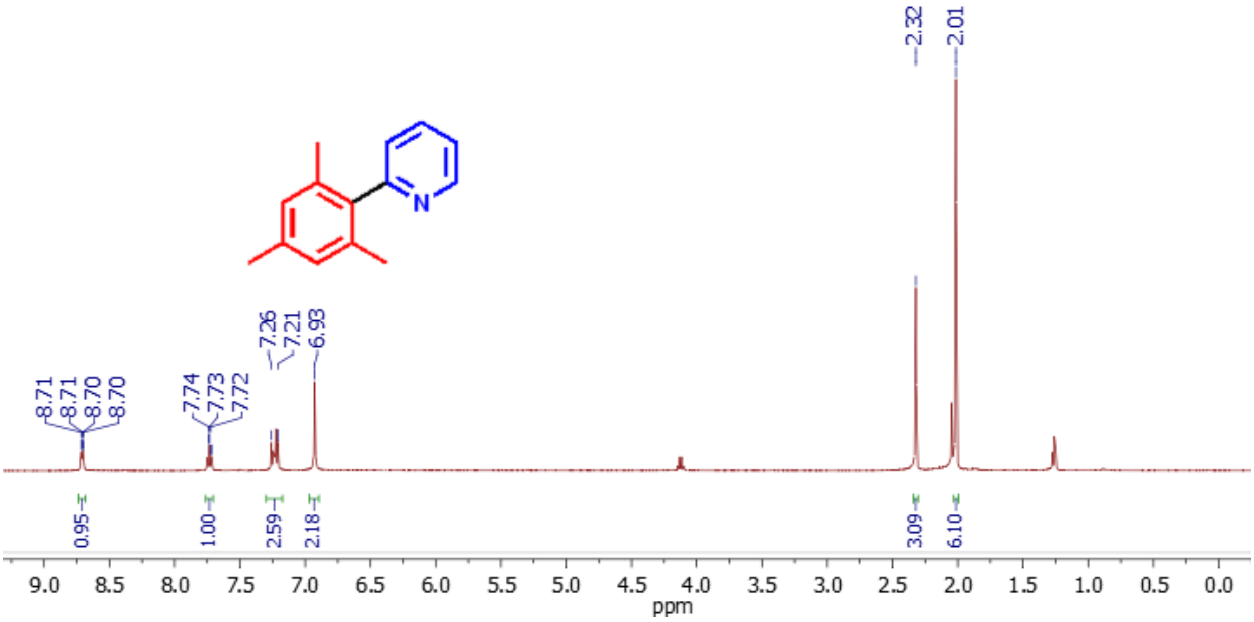

^{13}C – $CDCl_3$

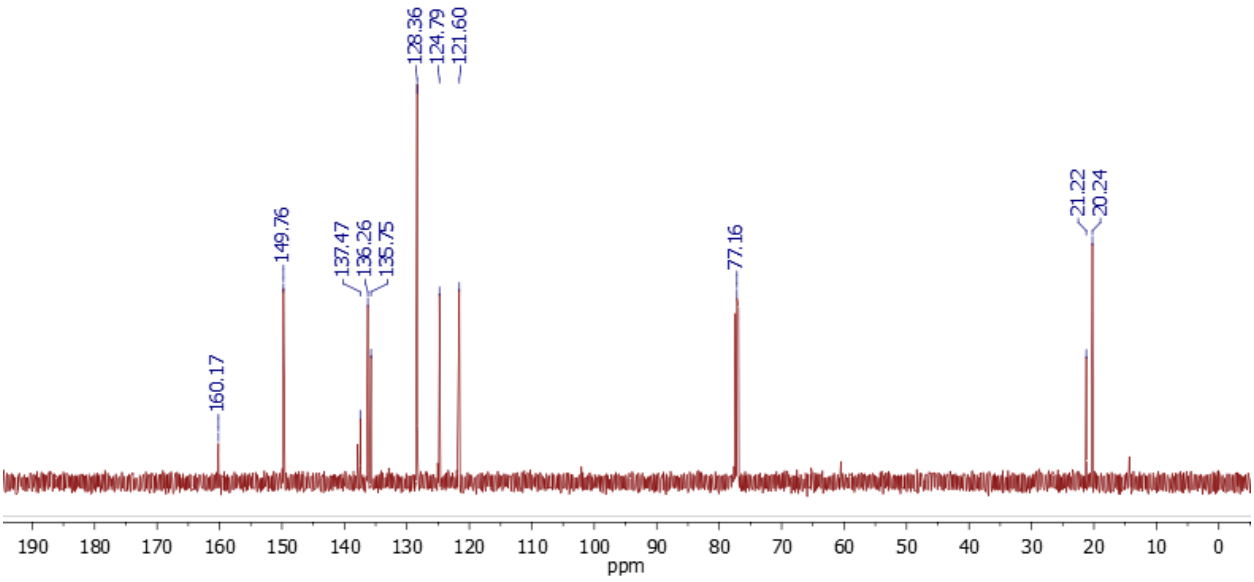

2-(2,4,6-triisopropylbenzyl)pyridine.

^{1}H NMR – $CDCl_3$

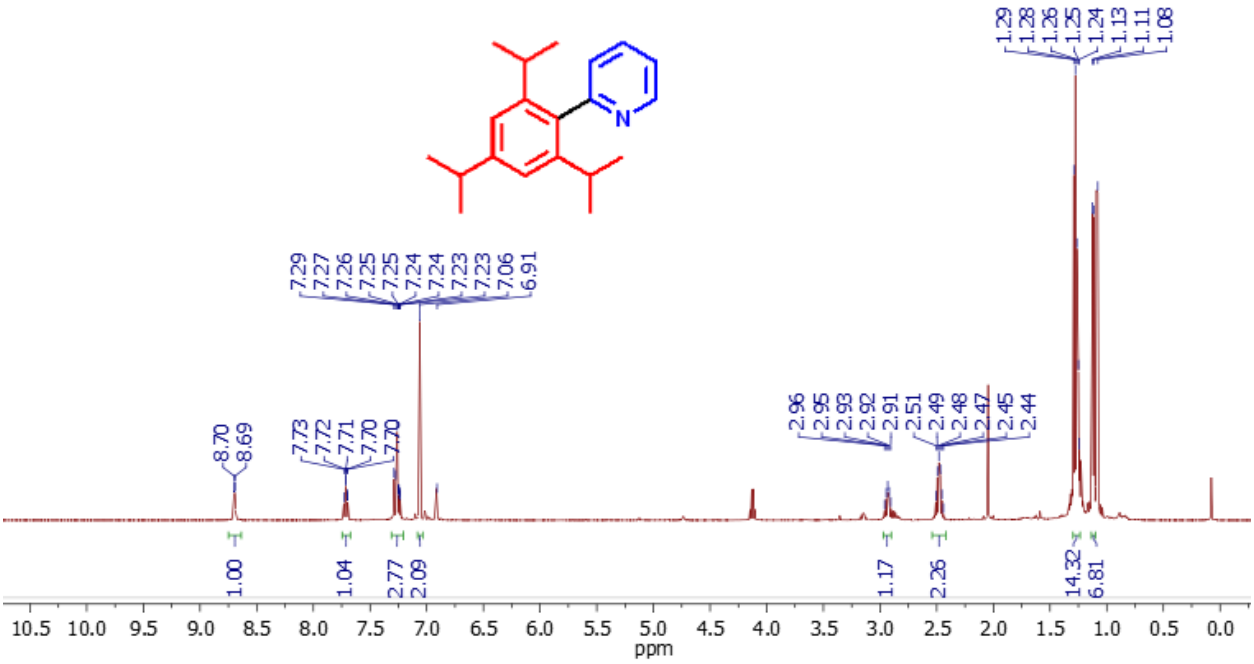

^{13}C – $CDCl_3$

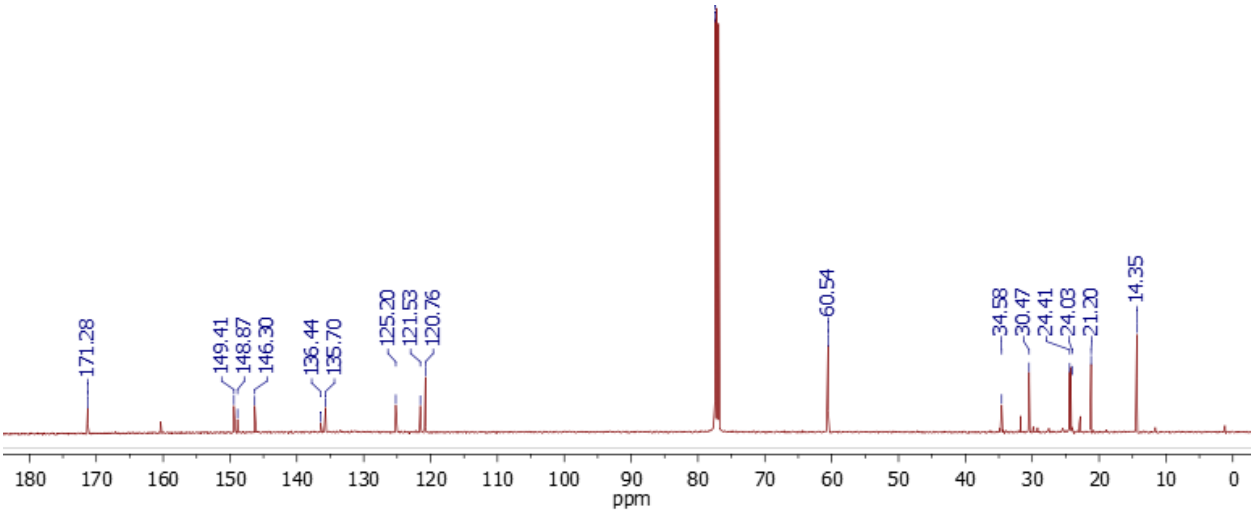

2.6.7 Crystallographic Data

Table 2.6: Crystallographic Parameters of (PN)$CoMes_2$.

Empirical formula	$C_{38}H_{42}CoNP$
Formula weight	602.62
Temperature/K	100.0
Crystal system	monoclinic
Space group	$P2_1/c$
a (Å)	12.1234(4)
b (Å)	14.2426(5)
c (Å)	19.1427(6)
α (°)	90
β (°)	105.6396(10)
γ (°)	90
Volume ($Å^3$)	3182.97(18)
Z	1
Radiation	MoKα (λ = 0.71073)
Reflections collected	46934
Independent reflections	5854 [R_{int} = 0.0513]
Goodness-of-fit on F^2	1.109
Final R indexes [I>=2σ (I)]	R_1 = 0.0350
	wR_2 = 0.0824
Final R indexes [all data]	R_1 = 0.0422 wR_2 = 0.0865

2.7 References

1. Fortman, G. C., Nolan, S. P. *N*-Heterocyclic Carbene (NHC) Ligands and Palladium in Homogeneous Cross-Coupling Catalysis: A Perfect Union. *Chem. Soc. Rev.* **2011**, *50*, 5151-5169.
2. Joshi-Pangu, A., Wang, C.-Y. & Biscoe, M. R. Nickel-Catalyzed Kumada Cross-Coupling Reactions of Tertiary Alkylmagnesium Halides and Aryl Bromides/Triflates. *J. Am. Chem. Soc.* **2011**, *133,* 84780-8481.
3. Sun, C., Krause, H., Fürstner, A. A Practical Procedure for Iron-Catalyzed Cross-Coupling Reactions of Sterically Hindered Aryl-Grignard Reagents with Primary Alkyl Halides. *Adv. Synth. Catal.* **2014**, *356*, 1281-1291.
4. García-Alvarez, M.; León, S.; Alemán, C.; Campos, J. L.; Muñoz-Guerra, S. Helical Nylons 3. Synthesis and Crystal Structure of Poly(B- L -Aspartate)S with Branched Alkyl Side Chains. *Macromolecules* **1998**, *31* (1), 124.
5. Mathis, G.; Bourg, S.; Aci-Sèche, S.; Truffert, J.-C.; Asseline, U. Synthesis and Properties of *2*'-O-neopentyl Modified Oligonucleotides. *Org*. *Biomol*. *Chem*. **2013**, *11* (8), 1345–1357.
6. Kharasch, M. S.; Fields, E.K. Factors Determining the Course and Mechanisms of Grignard Reactions. IV. The Effect of Metallic Halides on the Reaction of Aryl Grignard Reagents and Organic Halides. *J. Am. Chem. Soc.* **1941**, *63* (9), 2316-2320.
7. Kharasch, M. S.; Fuchs, C. F. Factors Determining the Course and Mechanisms of Grignard Reactions. XI. The Effect of Metallic Halides on the reaction of Grignard Reagents with Vinyl Halides and Substituted Vinyl Halides. *J. Am. Chem. Soc.* **1943**, *65* (4), 504-507.
8. Cahiez, G.; Moyeux, A. Cobalt-Catalyzed Cross-Coupling Reactions. *Chem. Rev.* **2010**, *110*, 1435-1462.
9. Brennan, M. R., Kim, D., Fout, A. R. A Synthetic and Mechanistic Investigation into the Cobalt(I) Catalyzed Amination of Aryl Halide. *Chem*. *Sci*. **2014**, *5*, 4831-4839.
10. Cahiez, G.; Chaboche, C.; Duplais, C.; Moyeux, A. A New Efficient Catalytic System for the Chemoselective Cobalt-Catalyzed Cross-Coupling of Aryl Grignard Reagents with Primary and Secondary Alkyl Bromides. *Org. Lett.* **2008**, *11* (2), 277–280.
11. Ohmiya, H., Yorimitsu, H., Koichiro, O. Cobalt(diamine)-Catalyzed Cross-Coupling Reaction of Alkyl Halides with Arylmagnesium Reagents: Stereoselective Constructions of Arylated Asymmetric Carbons and Application to Total Synthesis of AH13205. *J. Am. Chem. Soc.* **2006**, *128*, 1886-1889.
12. Collins, K. D.; Glorius, F. A Robustness Screen for the Rapid Assessment of Chemical Reactions. *Nature Chemistry* **2013**, *5* (7), 597.
13. Bagherzadeh, S.; Mankad, N. P. Extremely Efficient Hydroboration of Ketones and Aldehydes by Copper Carbene Catalysis. *Chem. Commun.* **2016**, *52* (19), 3844.
14. Hale, L. V. A.; Szymczak, N. K. Stereoretentive Deuteration of α-Chiral Amines with D2O. *J. Am. Chem. Soc.* **2016**, *138* (41), 13489.
15. Jia, Z., Liu, Q., Peng, X., Wong, H. N. C. Iron-catalysed Cross-Coupling of Organolithium Compunds with Organic Halides. *Nat. Comm.* **2016***, 7*, 10614.
16. Tasker, S. Z., Standley, E. A., Jamison, T. F. Recent Advances in Homogeneous Nickel Catalysis. *Nature*. **2014**, *509*, 299-309.
17. Li, J., Li, X., Sun, H. Synthesis and Characterization of Novel Organonickel and Organocobalt Complexes via Carbon-chlorine Bond Activation*. J. Organomet. Chem*. **2013**, *743*, 114-122.

CHAPTER 3: DEVELOPMENT AND METALATION OF A BIDENTATE CC LIGAND

3.1 Introduction

Interested in promoting the unique reactivity by first-row transition metals, we sought ligands which could provide an electron rich, strong field coordination environment. A monoanionic bis(carbene) ^{Ar}CCC ligand platform[1] (Ar = 1,3,5-trimethylphenyl (Mes) or 2,6-diisopropylphenyl (DIPP)) has been employed in cobalt complexes[2] that can be easily cycled between Co(I)-Co(III) oxidation states (**Figure 3.1a,b**), and have been applied to catalytic hydrogenation of terminal alkynes[3] as well as the anti-Markovnikov hydrosilylation of alkenes.[4] The CCC platform has also been able to support one of the first isolable Ni(IV) complexes via the oxidation of a Ni(II) using simple halogen surrogates (**Figure 3.1c**).[5] While interesting reactivity has been demonstrated both with (CCC)Co and (CCC)Ni complexes, the carbanion backbone exerts a strong *trans*-influence, resulting in unusual coordination geometries (**Figure 3.1b**) which, coupled with an inherently limited number of open coordination sites, may limit catalytic activity.

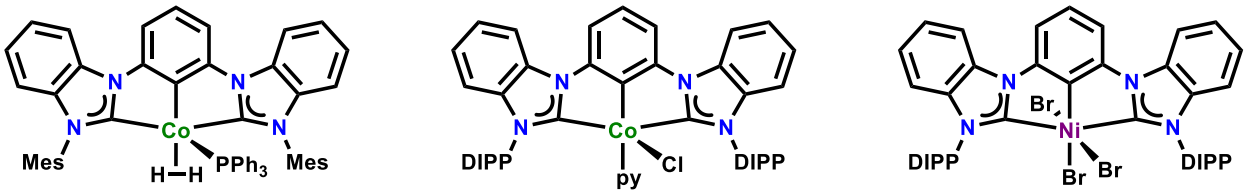

Figure 3.1: CCC complexes of cobalt[2] (a, b) and nickel[5] (c).

In pursuit of even more catalytically active metal complexes, we sought a bidentate CC ligand featuring both an *N*-heterocyclic carbene and anionic C_{aryl} coordination, which may be able to confer the stabilization and strong field environment provided by the CCC platform balanced with the high reactivity observed by the low-coordinate cobalt complexes.[6] Metal complexes with bidentate ligand coordination, including bis(amine) ligands such as phen and TMEDA, a huge

library of phosphine chelators, and even some work using bis-NHC ligands, as well as mixed-donor species, are ubiquitous in catalysis and used to tackle a diverse array of chemical syntheses.[7] A greater number of open coordination sites could offer improved reactivity over the pincer CCC platform by allowing *cis*-substitution of substrates on the metal center in conformations which avoid the *trans*-influence of the carbanion moiety, promoting oxidative addition and reductive elimination pathways.

3.2 Ligand Development

A new, bidentate CC ligand was designed containing only a single imidazole arm. Imidazole was selected over benzimidazole for synthetic ease. While metalation of the CCC ligand involves activation of a C_{aryl}–H bond on the backbone a 2-bromo-substituted aryl ring was chosen for the CC to facilitate cyclometalation. The aryl ring was also substituted with *tert*-butyl groups for improved solubility, and to add steric bulk to the ligand.

Synthesis of 1-arylimidazoles[8] (aryl = 2,4,6-trimethylphenyl- (Mes) (**1a**) or 2,6-diisopropylphenyl- (DIPP)(**1b**)) and 2-bromo-3,5-di-*tert*-butyl-1-bromomethyl benzene[9] (**2**) were carried out following literature methods. Reflux of **1a** or **1b** with **2** in toluene for 4 hours resulted in nucleophilic substitution to form asymmetric imidazolium bromide salts H(^{Mes}CC)Br (**3**) and H(^{DIPP}CC)Br (**4**) in 92-94% yield (**Scheme 3.1**). The formation of the desired products was confirmed by observation of the resonance corresponding to the imidazolium C–H in the ^{1}H NMR spectrum in $CDCl_3$, appearing at 10.29 ppm and 10.20 ppm for **3** and **4**, respectively.

As coordination of NHC ligands requires deprotonation of the corresponding imidazolium salt, it was desirable to demonstrate that the carbene form of the CC ligand could be generated and assess its stability. Stirring **3** or **4** in THF or toluene with one equivalent of lithium

bis(trimethylsilyl)amide ($LiN(SiMe_3)_2$) resulted in dissolution of the ligand salt to form a light yellow solution, as well as disappearance of the aforementioned C–H resonance as observed by ^1H NMR spectroscopy, indicating formation of the NHC species. The NHC form of each ligand seems to be reasonably stable, with no significant change in the ^1H NMR spectrum after 24 h at room temperature in C_6D_6 or THF-d_8. Other bases such as NaH and $NaHBEt_3$ could also cleanly generate the NHC, though reaction with carbanion bases such as benzyl potassium and trimethylsilylmethyllithium ($LiCH_2SiMe_3$) resulted in decomposition of the ligand salt to uncharacterized diamagnetic products.

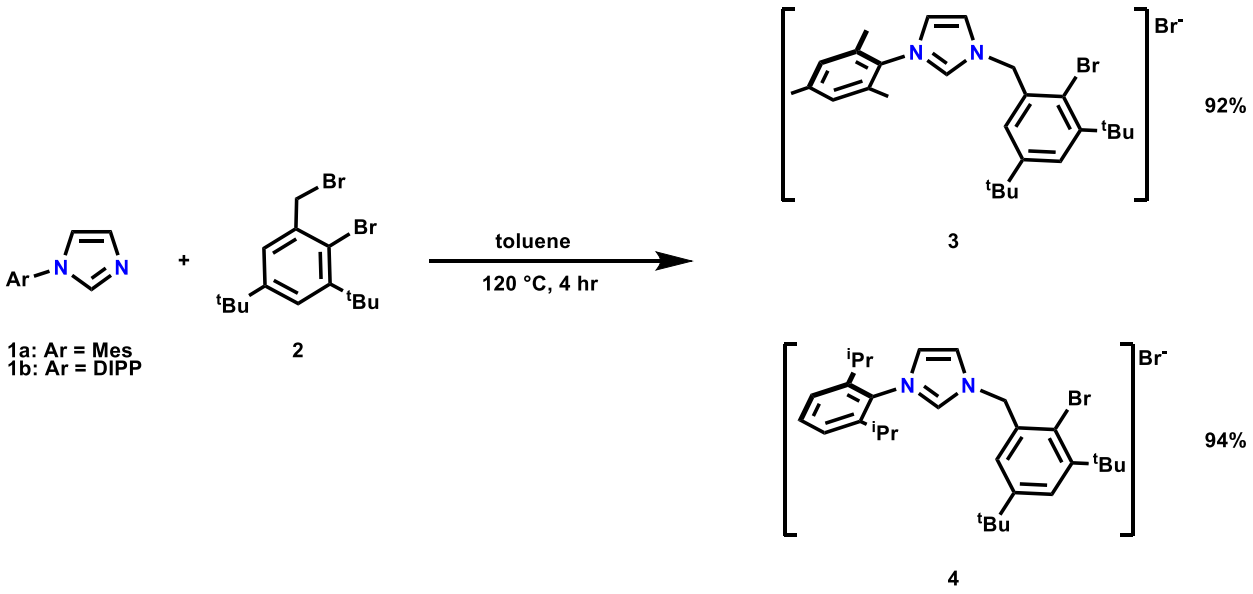

Scheme 3.1: Synthesis of CC ligands.

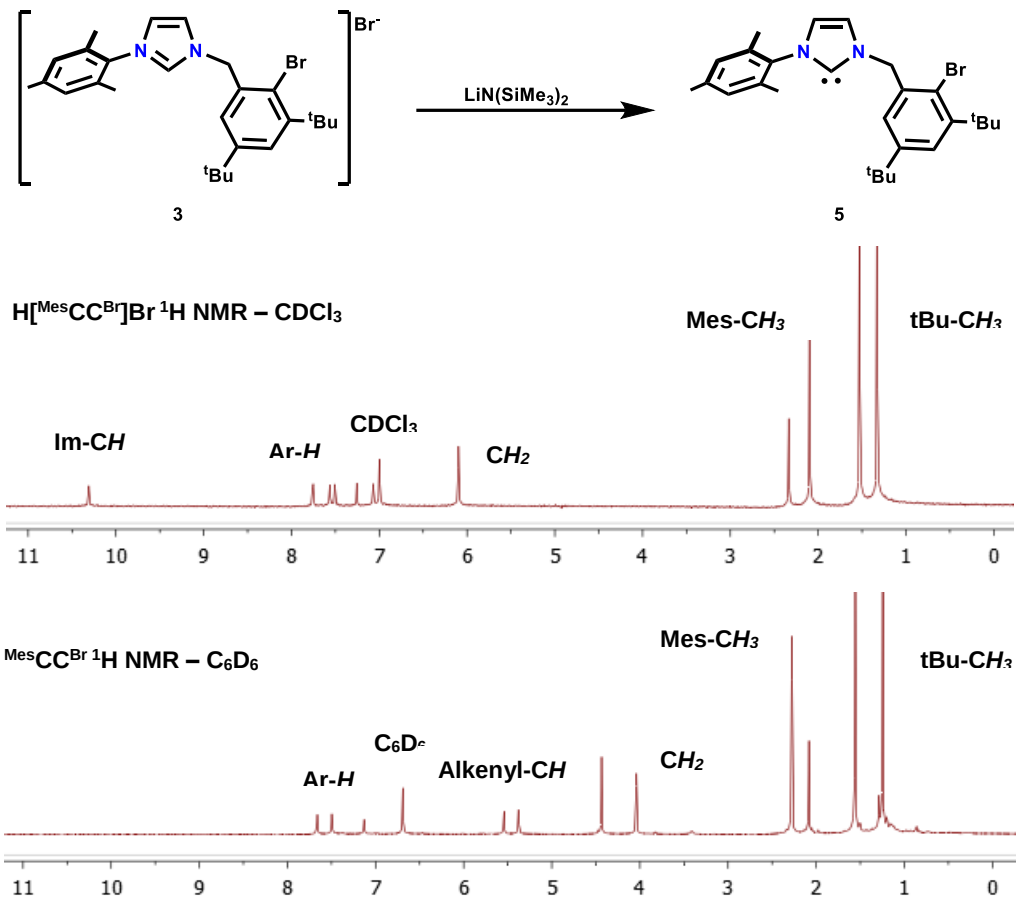

Figure 3.2: Formation of the NHC $^{Mes}CC^{Br}$.

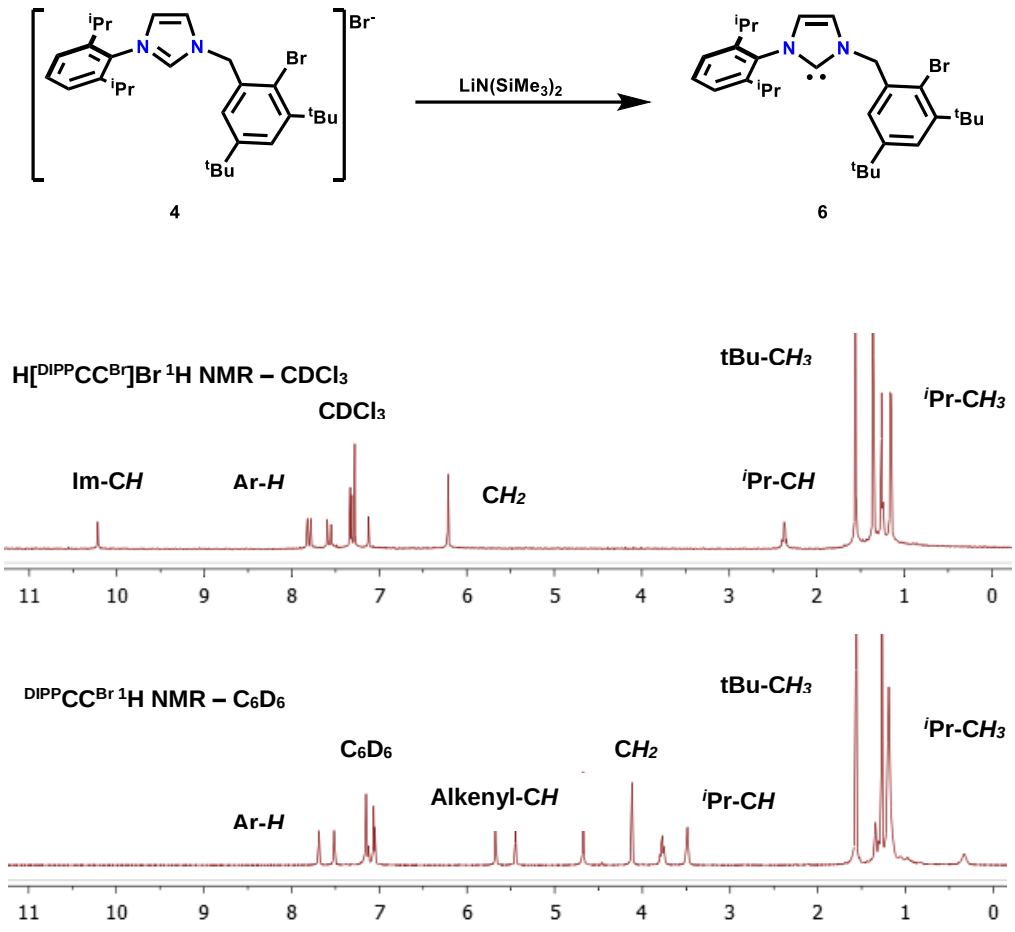

Figure 3.3: Formation of the NHC $^{DIPP}CC^{Br}$.

3.3 Metalation with Cobalt

At present, there are only two examples of cobalt complexes featuring bidentate CC coordination; one with a dianionic bis-aryl chelating ligand on a coordinatively saturated cobalt center,[10] and a homoleptic species coordinating two equivalents of IMes in which a benzylic C–H bond has been activated on one of the mesityl flanking groups of each ligand (**Figure 3.4**).[11]

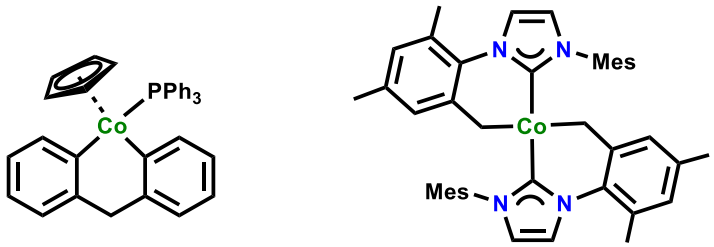

Allison Deng

Figure 3.4: Bidentate CC cobalt complexes.

Inspired by metalation strategies employed for (CCC)Co complexes in our group, **3** was treated with $Co(PPh_3)_2Br_2$ followed by 1 equiv. $LiN(SiMe_3)_2$, in an attempt to generate complex **7** (**Figure 3.5**). It was hypothesized that addition of reductant to this species could form the cyclometalated CC complex by reduction of the cobalt center with subsequent oxidative addition onto the C_{aryl}–Br bond. Upon treatment with KC_8, a light blue paramagnetic product was isolated (as evidenced by ^1H NMR). Crystals were grown and used to identify connectivity by X-ray diffraction, indicating the formation of a bis-NHC cobalt dibromide species. Treatment of **3** with $CoBr_2$ in the presence of various L type ligands (PPh_3, PMe_3, pyridine) and a single equivalent of base did not prevent the formation of the bis-NHC cobalt species. Inclusion of KC_8 in the reaction mixture did not achieve the desired C–Br activation. Treatment of **8** with KC_8 directly also failed to yield the cobalt complex bound in the desired bidentate fashion. Complex **8** may warrant further study, as cobalt bis-NHC complexes have been shown to exhibit interesting stoichiometric reactivity;[12] however, there was no immediately apparent pathway from this species to a cobalt complex coordinated to a single C–C chelating ligand.

Attempts at metalation of ^{DIPP}CC using the above procedures furnished an analogous bis-NHC complex; however, use of limiting $NaHBEt_3$ as a base followed by $Co(PPh_3)_2Br_2$ results in a color change to green and then to light blue, forming a species distinct

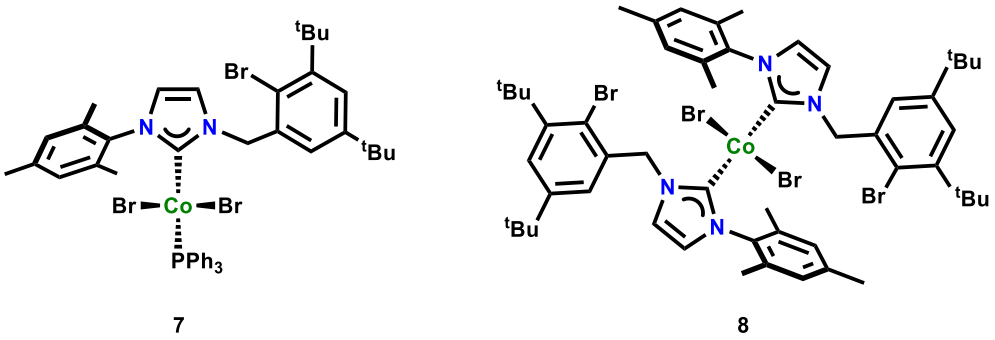

7 8

Figure 3.5: Proposed structure of (^{Mes}CC)Co(PPh$_3$)Br$_2$ (**7**), and (^{Mes}CC)$_2$CoBr$_2$ (**8**) as identified by connectivity using X-ray crystallography.

from the bis-NHC complexes by ^{1}H NMR spectroscopy. Ito and coworkers[13] reported the deprotonation of imidazolium complexes with LiHBEt$_3$ resulting in a stable borane-NHC adduct; deprotonation of H(^{DIPP}CC)Br with NaHBEt$_3$ likely results in an analogous NHC-BEt$_3$ adduct. This adduct was evidenced by a resonance at -16.9 ppm in the ^{11}B NMR spectrum, as compared to reported shift of IMes•BEt$_3$ (-13.3 ppm) and a significant shift from BEt$_3$ (86.7 ppm). It is possible that coordination of the borane inhibits the formation of the bis-NHC cobalt complex sufficiently to result in a DIPP analogue of proposed complex **7**. However, X-ray diffraction identified the product as the imidazolium salt [H(^{DIPP}CC)][Co(PPh$_3$)Br$_3$] (**Figure 3.6**).

To attempt to circumvent the problems associated with C–Br cleavage by cobalt to metalate, activation of the aryl ring by lithium-halogen exchange was attempted by treatment of **3** with *n*-butyllithium after generation of the NHC as described above. However, a stable lithiated species could not be isolated, and metalation by *in situ* lithium-halogen exchange followed by addition of cobalt sources was similarly unproductive. Efforts to insert magnesium into the C–Br bond was likewise unsuccessful at formation of a stable activated species or assisting coordination of the ligand to cobalt. Inability to undergo these exchanges may be due in part to other electron deficient C–H bonds in the molecule such as those on benzylic positions of the mesityl group and on the methylene linker that are potentially sensitive to strong bases.

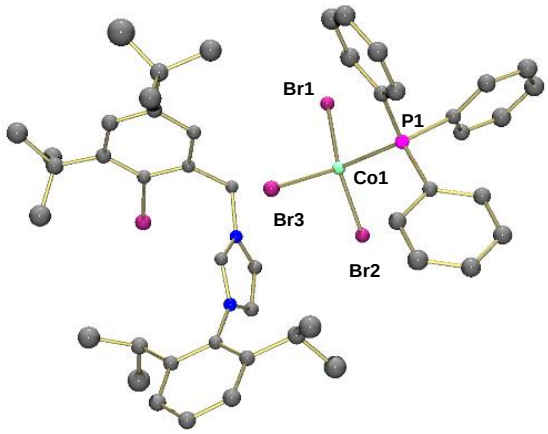

Figure 3.6: X-ray crystal structure of [H(^{DIPP}CC)][Co(PPh_3)Br_3] depicted with 50% probability ellipsoids. Solvent molecules and H atoms have been omitted for clarity. Selected bond distances (Å) and angles (°): Co1–Br1 2.4009(9), Co1–Br2 2.3851(9), Co1–Br3 2.3728(10), Co1–P1 2.3716(17), P1–Co1–Br1 104.00(5), P1–Co1–Br2 111.02(5), P1–Co1–Br3 106.16(5).

The core challenge in developing a metalation strategy to bind cobalt to a single CC ligand in bidentate fashion remains somewhat unclear, as recent work in our group has led to the synthesis of a series of bidentate CC nickel(II) complexes using the same ligand platform.[14] It is possible that in this environment the necessary C–Br bond activation is too challenging, though there are examples of comparable intramolecular C–X bond cleavage by cobalt in the literature.[15] Perhaps more likely is that single NHC cobalt species are unstable and/or are prone to rapidly form very stable complexes in which the NHC from two different ligands is bound.

3.4 NCC Ligand

A pincer ligand alternative to the CC has been developed which replaces the DIPP/Mes substituent with a 5-methylpyridyl moiety. Chelation to the metal at the pyridyl and NHC sites was hypothesized to promote formation of a single-ligand metal complex by offering improved

stabilization; the resulting complex could then be carried forward to C–Br activation and cyclometalation. While this ligand platform does not provide as many open coordination sites as ^{Ar}CC, it should still allow for *cis*-coordination of substrates free of the *trans*-influence of the carbanion. Synthesis of 1-picolyl-imidazole was carried out by literature methods,[16] followed by nucleophilic substitution in the same manner as ^{Ar}CC ligands to form H(NCC)Br (**9**), and in comparable yield (**Scheme 3.2**).

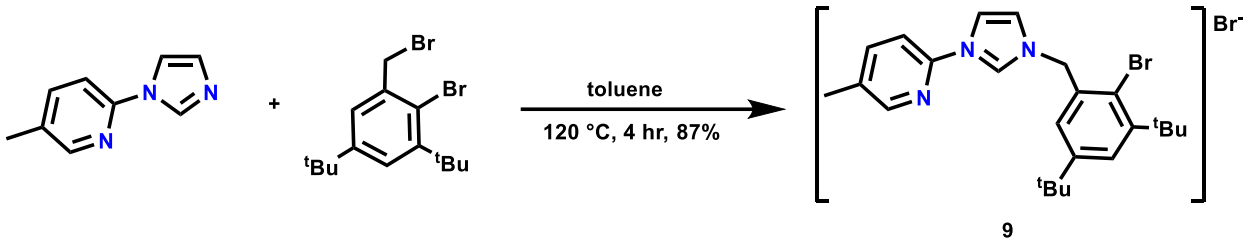

Scheme 3.2: Synthesis of H(NCC)Br.

A substantial decrease in solubility relative to **3** and **4** was observed both in regard to **9** and products of reactions with transition metals. Treatment with bases such as $LiN(SiMe_3)_2$ and $NaHBEt_3$ resulted in loss of the imidazolium C–H resonance in the ^{1}H NMR spectrum, though the NHC could not be cleanly isolated, indicating a relative lack of stability as compared to the other CC ligands.

3.5 NCC Metalation

Many of the strategies employed to metalate the previously mentioned CC ligands were also employed towards NCC. In general, reaction of **9** with base in the presence of Co(II) salts resulted in products which were highly insoluble, severely limiting characterization or further manipulation. Inclusion of external reductant such as KC_8 in the reaction mixture only resulted in complex mixtures of paramagnetic species. Use of the above Co(I), Co(0), and Co(I-) species

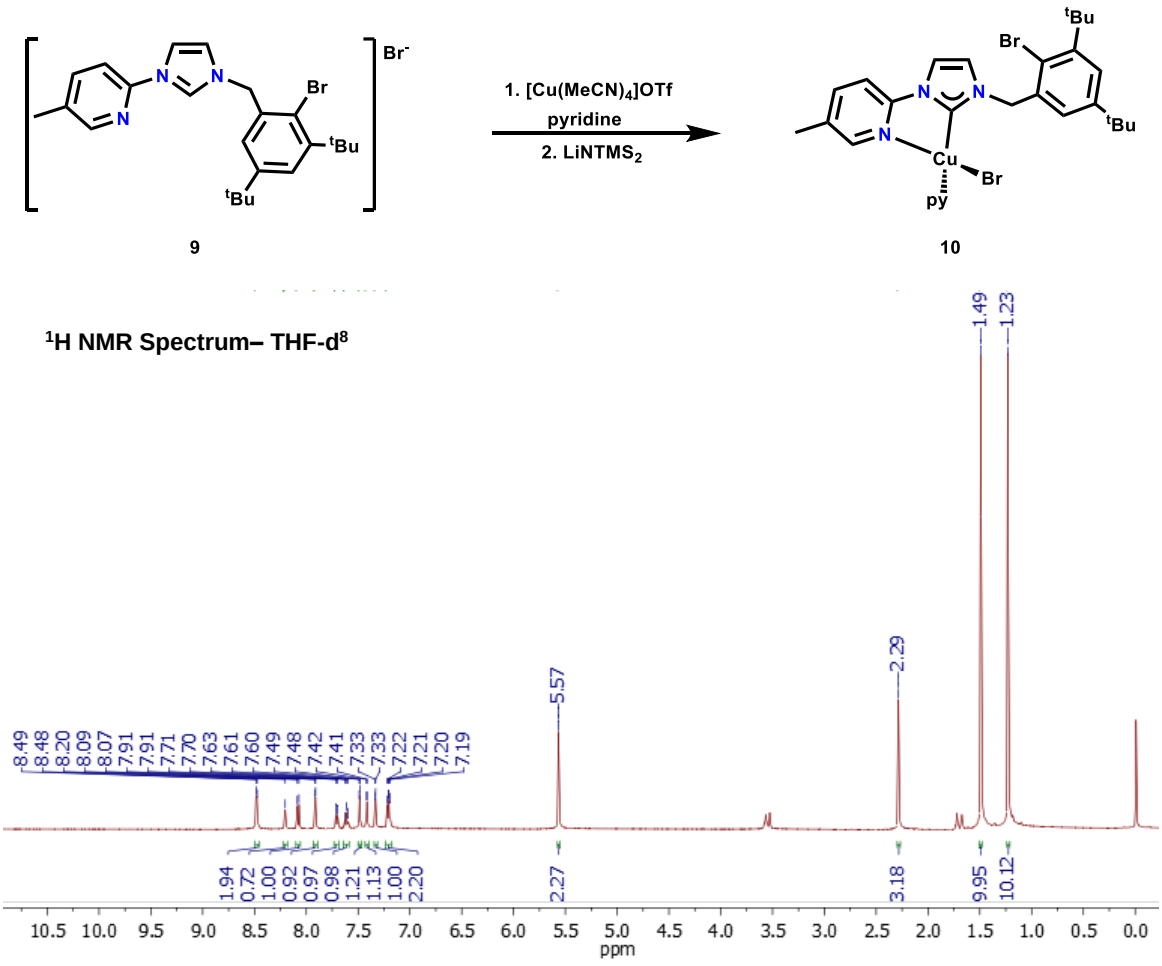

Figure 3.7: Reaction of NCC with $[Cu(MeCN)_4]OTf$.

produced similarly unproductive results. Interestingly, treatment of a mix of NCC and $[Cu(MeCN)_4]OTf$ with base produced a stable, light yellow diamagnetic solid. After thorough washing with hexanes and drying under vacuum, the ^1H spectrum integrates to one equivalent of pyridine relative to ligand, which has shifted from ligand salt and lost the imidazolium C–H resonance. This species is proposed to be a four-coordinate copper(I) complex binding the NHC and pyridine sites of the NCC (**Figure 3.7**). However, efforts to activate the C_{aryl}–Br bond by copper or *n*-butyllithium have been unsuccessful thus far.

3.6 Summary

A series of asymmetric imidazolium salts inspired by the CCC ligands were synthesized to develop a class of bidentate CC ligands in hopes of providing a unique coordination environment and promote interesting metal reactivity. The propensity of cobalt to bind two NHC ligands coupled with the difficulty of activating the C_{aryl}–Br bond has made the synthesis of stable cyclometalated cobalt complexes using the CC ligands difficult. Such issues have thus far prevented any exploration of the ligand's potential utility in stoichiometric reactivity and catalysis. The problems encountered in metalation may explain the relative dearth of chelating CC cobalt complexes in the literature. Similar work in our group using nickel suggest that the C_{aryl} coordination site is more exposed than in CCC complexes, leaving it more vulnerable to insertion-type chemistry. This feature could ultimately inhibit its applicability in catalysis.

3.7 Experimental

3.7.1 General Considerations

All manipulations of metal complexes were carried out in the absence of water and dioxygen using standard Schlenk techniques, or in an MBraun inert atmosphere drybox under a dinitrogen atmosphere except where otherwise specified. All glassware was oven dried for a minimum of 8 h and cooled in an evacuated antechamber prior to use in the drybox. Diethyl ether, tetrahydrofuran, toluene and benzene were dried and deoxygenated on a Glass Contour System (SG Water USA, Nashua, NH) and stored over 4 Å molecular sieves (Strem) prior to use. Chloroform-*d* and Benzene-d_6 were purchased from Cambridge Isotope Labs and were degassed and stored over 4 Å molecular sieves prior to use. 1-bromo-2-(bromomethyl)-4,6,-di-*tert*-butylbenzene and 1-arylimidazoles were prepared following literature methods.[7,8,15] Cobalt salts,

pyridine, NaH, $NaHBEt_3$, and tetrakisacetonitrile copper(I) triflate were purchased from Sigma-Aldrich and used as received. Triphenylphosphine and $LiN(SiMe_3)_2$ were each purchased from Sigma-Aldrich and recrystallized in concentrated hexanes prior to use. $Co(PMe_3)_4$, and $K[Co(PMe_3)_4]$ were prepared following literature methods.[17] Celite® 545 (J. T. Baker) was dried in a Schlenk flask for 24 hr under dynamic vacuum while heating to at least 150˚C prior to use in a drybox. NMR Spectra were recorded at room temperature on a Varian spectrometer operating at 500 MHz (^{1}H NMR) and 126 MHz (^{13}C NMR) and referenced to the residual $CHCl_3$ or C_6H_6 resonance (δ in parts per million, and *J* in Hz). Mass spectrometry (MS) was performed by the University of Illinois Mass Spectrometry Laboratory. Data are reported in the form of m/z (intensity relative to the base peak = 100).

3.7.2 Ligand Syntheses

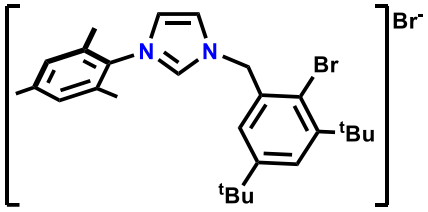

H(^{Mes}*CC*^{Br}*)Br.* A screw-top, thick-walled glass bomb was charged with 1-mesitylimidazole (0.54 g, 2.89 mmol), 1-bromo-2-(bromomethyl)-4,6,-di-*tert*-butylbenzene (1.05 g, 2.89 mmol), and 4 mL toluene. The bomb was sealed and heated at 130°C with stirring for 4 h. Upon cooling to room temperature, the resulting precipitate was collected by filtration and washed thoroughly with hexanes to yield a solid which ranged from white to beige in color. The product could be washed with ~15 mL THF and recrystallized from DCM/Hexanes to remove remaining brown color and yield white solid (1.46 g, 2.66 mmol, 92%). ^{1}H NMR (500 MHz, Chloroform-*d*) δ 10.32 (s, 1H), 7.77 (s, 1H), 7.57 (s, 1H), 7.51 (s, 1H), 7.07 (s, 1H), 7.00 (s, 2H), 6.11 (s, 2H), 2.34 (s, 3H), 2.11

(s, 6H), 1.54 (s, 9H), 1.33 (s, 9H); ^{1}H NMR (500 MHz, Chloroform-*d*) δ 151.57, 149.12, 141.51, 138.46, 134.49, 133.85, 130.81, 128.48, 127.20, 122.75, 122.62, 122.19, 56.13, 37.72, 35.17, 31.39, 30.15, 21.24, 17.88. HRMS (ESI^{+}) calcd for $C_{27}H_{36}BrN_2^{+}$ [M]$^{+}$: 467.2062, found: 467.2067.

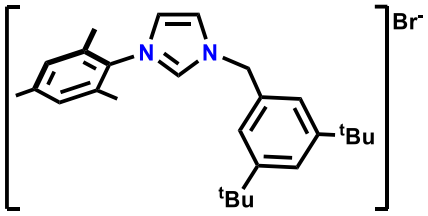

H(^{Mes}*CC*^{H}*)Br.* A screw-top, thick-walled glass bomb was charged with 1-mesitylimidazole (0.66 g, 5.5 mmol), 1-(bromomethyl)-3,5,-di-*tert*-butylbenzene (1.0 g, 5.5 mmol), and 4 mL toluene. The bomb was sealed and heated at 130°C with stirring for 4 h. Upon cooling to room temperature, the resulting precipitate was collected by filtration and washed thoroughly with hexanes to yield a solid which ranged from white to beige in color. The product could be washed with ~15 mL THF and recrystallized from DCM/Hexanes to remove remaining brown color and yield white solid (1.49 g, 90%). ^{1}H NMR (500 MHz, Chloroform-*d*) δ 10.77 (s, 1H), 7.45 (s, 1H), 7.38 (s, 1H), 7.23 (s, 2H), 7.09 (s, 1H), 7.02 (s, 2H), 5.94 (s, 2H), 2.35 (s, 3H), 2.12 (s, 6H), 1.31 (s, 18H); ^{13}C NMR (126 MHz, Chloroform-*d*) δ 152.37, 141.54, 139.59, 134.34, 132.59, 130.81, 130.04, 123.45, 123.07, 122.90, 122.58, 54.67, 35.11, 31.53, 21.24, 17.81. HRMS (ESI^{+}) calcd for $C_{27}H_{37}N_2^{+}$ [M]$^{+}$: 389.2957, found: 389.2956.

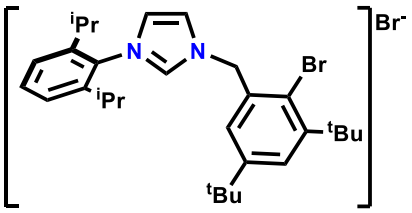

H(^{DIPP}*CC*^{Br}*)Br.* A screw-top, thick-walled glass bomb was charged with 1-(2,6-diisopropylphenyl)imidazole (0.662 g, 2.9 mmol), 1-bromo-2-(bromomethyl)-4,6-di-*tert*-butylbenzene (1.05 g, 2.9 mmol), and 4 mL toluene. The bomb was sealed and heated at 130°C with stirring for 4 h. Upon cooling to room temperature, the resulting precipitate was collected by filtration and washed thoroughly with hexanes to yield a solid which ranged from white to beige in color. The product could be washed with ~15 mL THF and recrystallized from DCM/Hexanes to remove remaining brown color and yield white solid (1.61 g, 94%). ^{1}H NMR (500 MHz, Chloroform-*d*) δ 10.20 (s, 1H), 7.80 (d, *J* = 2.5 Hz, 1H), 7.76 (m, 1H), 7.57 (d, *J* = 2.5 Hz, 1H), 7.53 (t, *J* = 8 Hz, 1H), 7.31 (d, *J* = 8 Hz, 2H), 7.10 (m, 1H), 6.19 (s, 2H), 2.35 (sept, *J* = 6.5 Hz, 2H), 1.54 (s, 9H), 1.33 (s, 9H), 1.24 (d, *J* = 7 Hz, 6H), 1.14 (d, *J* = 6.5 Hz, 6H); ^{13}C NMR (126 MHz, Chloroform-*d*) δ 151.64, 149.13, 145.59, 138.37, 134.00, 132.07, 130.27, 128.41, 127.19, 124.85, 123.85, 122.97, 122.12. HRMS (ESI^{+}) calcd for $C_{30}H_{42}BrN_2^{+}$ [M]$^{+}$: 509.2531, found: 509.2687.

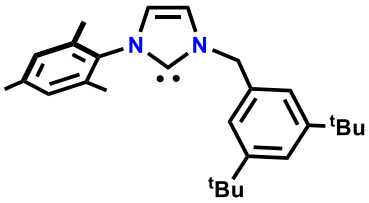

MesCC^{H}*.* H(^{Mes}CC^{H})Br (47 mg, 0.1 mmol) was combined with 2 mL THF and cooled to -30°C. A chilled solution of $LiN(SiMe_3)_2$ (18 mg, 0.11 mmol) in THF was added dropwise to the suspension, which dissolved rapidly into a clear solution. Solvent was removed *in vacuo* and the

residue was extracted with hexanes. Removal of volatiles yielded a light yellow waxy solid (37 mg, 95%). The free carbene is stable for more than 24 hours at room temperature under N_2 atmosphere, though it was typically generated *in situ* for metalation experiments. ^{1}H NMR (500 MHz, C_6D_6) δ 7.47 (s, 1H), 7.29 (s, 2H), 6.79 (s, 2H), 6.34 (bs, 1H), 6.05 (bs, 1H), 5.54 (s, 2H), 2.14-2.11 (m, 9H), 1.35 (s, 18H).

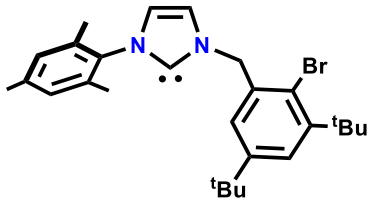

$^{Mes}CC^{Br}$. H($^{Mes}CC^{Br}$)Br (55 mg, 0.1 mmol) was combined with 2 mL THF and cooled to -30°C. A chilled solution of $LiN(SiMe_3)_2$ (18 mg, 0.11 mmol) in THF was added dropwise to the suspension, which dissolved rapidly into a clear solution. Solvent was removed *in vacuo* and the residue was extracted with hexanes. Removal of volatiles yielded a light yellow waxy solid (45 mg mg, 97%). The free carbene is stable for more than 24 hours at room temperature under N_2 atmosphere, though it was typically generated *in situ* for metalation experiments. ^{1}H NMR (500 MHz, C_6D_6) δ 7.70 (d, *J* = 2 Hz, 1H), 7.53 (d, *J* = 2.5 Hz, 1H), 6.72 (s, 2H), 5.58 (d, *J* = 2.5 Hz, 1H), 5.41 (d, *J* = 2.5 Hz, 1H), 4.07 (s, 2H), 2.31 (s, 6H), 2.11 (s, 3H), 1.59 (s, 9H), 1.27 (s, 9H).

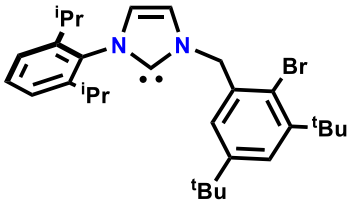

$^{DIPP}CC^{Br}$. H($^{DIPP}CC^{Br}$)Br (59 mg, 0.1 mmol) was combined with 2 mL THF and cooled to -30°C. A chilled solution of $LiN(SiMe_3)_2$ (17 mg, 0.11 mmol) in THF was added dropwise to the suspension, which dissolved rapidly into a clear solution. Solvent was removed *in vacuo* and the residue was extracted with hexanes. Removal of volatiles yielded a light yellow waxy solid (49 mg, 97%). The free carbene is stable for more than 24 hours at room temperature under N_2 atmosphere, though it was typically generated *in situ* for metalation experiments. ^{1}H NMR (500 MHz, C_6D_6) δ 7.70 (s, 1H), 7.52 (s, 1H), 7.07 (m, 1H), 7.06 (bs, 1H), 5.69 (s, 1H), 5.45 (s, 1H), 4.68 (s, 2H), 3.78 (sept, *J* = 7 Hz, 2H), 1.57 (s, 9H), 1.28 (s, 9H), 1.20 (bs, 12H).

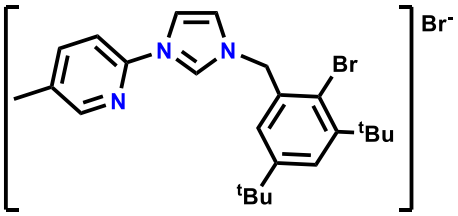

H(NCC)Br. A screw-top, thick-walled glass bomb was charged with 1-(4-methylpyridyl)imidazole (318 mg, 2 mmol), 1-bromo-2-(bromomethyl)-4,6-di-*tert*-butylbenzene (742 mg, 2 mmol), and 4 mL toluene. The bomb was sealed and heated at 130°C with stirring for 4 h. Upon cooling to room temperature, the resulting precipitate was collected by filtration and washed thoroughly with hexanes to yield a solid which ranged from white to beige in color. The product could be washed with ~15 mL THF and recrystallized from DCM/Hexanes to remove remaining brown color and yield white solid (922 g, 87%). ^{1}H NMR (500 MHz, Chloroform-*d*) δ 11.94 (s, 1H), 8.50 (d, *J* = 8.5 Hz, 1H), 8.29 (s, 1H), 8.16 (m, 1H), 7.85-7.83 (dd, *J* = 8.5, 1.5 Hz,

1H) 7.81 (d, *J* = 2.5 Hz, 1H), 7.58 (d, *J* = 2 Hz, 1H), 7.35 (m, 1H), 5.91 (s, 2H), 2.42 (s, 3H), 1.54 (s, 9H), 1.35 (s, 9H); ^{13}C NMR (126 MHz, Chloroform-*d*) δ 151.83, 149.15, 149.03, 144.15, 141.14, 136.10, 135.57, 133.49, 128.49, 127.51, 122.27, 122.27, 121.83, 118.42, 114.97. HRMS (ESI$^+$) calcd for $C_{24}H_{31}BrN_3$ [M]$^+$: 440.1701, found: 440.1701.

3.7.3 Metal Complex Syntheses

$Co(PPh_3)_2Br_2$ (adapted from literature methods[18] to be performed inside a glovebox). A 20mL vial was charged with $CoBr_2$ (125 mg, 0.57 mmol) and PPh_3 (300 mg, 1.14 mmol) and 5 mL THF was added. The dark blue solution was heated to 60°C while stirring for 20 minutes, followed by 3 hours of stirring while cooling to room temperature. Solvent was removed, and the residue was washed with hexanes (3 x 2 mL) to yield a blue-green solid (382 mg, 90%). ^{1}H NMR (500 MHz, C_6D_6) δ 15.07, -3.59, -5.08.

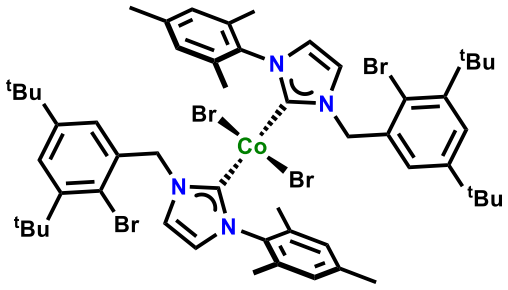

(^{Mes}CC)$CoBr_2$. In a glovebox, a 20 mL vial was charged with H(^{Mes}CC)Br (110 mg, 0.40 mmol) and $CoBr_2$ (44 mg, 0.20 mmol), dissolved in ~3 mL THF (very little of H(^{Mes}CC)Br will dissolve), and cooled to -35°C. $LiN(SiMe_3)_2$ (33.5 mg, 0.20 mmol) was weighed into a separate vial and cooled to -35°C. $LiN(SiMe_3)_2$ was added dropwise to the ligand/metal mixture while stirring, during which H(^{Mes}CC^X)Br slowly dissolved as it reacted. The light blue solution was stirred

for 1 h. Solvent was removed *in vacuo* and washed with hexanes (3 x 2 mL) to yield a light blue solid (159 mg, 69 %). ^{1}H NMR (500 MHz, C_6D_6) δ 44.13, 37.83, 9.57, 4.34, 1.32, 0.11, -7.81.

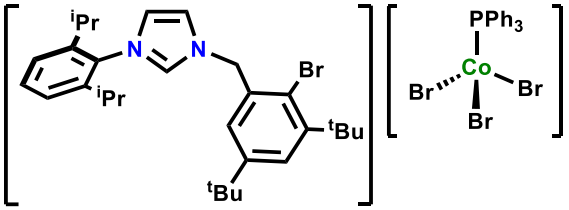

[H(^{DIPP}CC)][Co(PPh$_3$)Br$_3$]. A 20 mL scintillation vial was charged with H(^{DIPP}CC)Br (50 mg, 0.084 mmol) and Co(PPh$_3$)$_2$Br$_2$ (63 mg, 0.085 mmol). 3 mL THF was added and the mixture cooled to -35°C. To the light blue mixture NaHBEt$_3$ (1.0 M in toluene, 0.084 mL, 0,084 mmol) was added dropwise. H(^{DIPP}CC)Br dissolved as NaHBEt$_3$ was added, and color change to green was observed, followed quickly by change again to light blue. Solvent was removed *in vacuo* to give a waxy blue solid, which was dissolved in dichloromethane (DCM). Layering of hexanes over a concentrated solution of the product in DCM produced light blue crystals suitable for X-ray crystallographic analysis (69 mg, 77%). ^{1}H NMR (500 MHz, C_6D_6) δ 13.79, 6.82, 5.92, 2.29, 1.92, 0.44, -1.02, -2.24, -4.23, -8.35, -12.02.

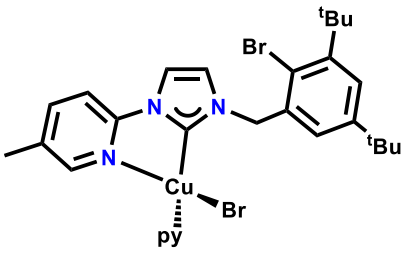

(NCC)Cu(py)Br (proposed). A 20 mL vial was charged with H(NCC)Br (51 mg, 0.1 mmol), [Cu(MeCN)$_4$][OTf] (38 mg, 0.1 mmol). 3 mL THF was added, followed by pyridine (12 mg, 0.15

mmol). The mixture was cooled to -35°C, and $NaHBEt_3$ (1.0 M in toluene, 0.11 mL, 0.11 mmol) was added slowly to give a light yellow solution. Solvent was removed *in vacuo* and the resulting residue was washed with hexanes (3 x 2 mL) to yield a light yellow solid (47 mg, 81%). ^{1}H NMR (500 MHz, THF-d^8) δ 8.48 (d, *J* = 4.5 Hz, 2H), 8.20 (s, 1H), 8.08 (d, *J* = 8 Hz, 1H), 7.91 (d, *J* = 2 Hz, 1H), 7.70 (d, *J* = 8 Hz, 1H), 7.61 (dt, *J* = 7.5 Hz, 1.5 Hz, 1H), 7.48 (d *J* = 2.5 Hz, 1H), 7.41 (d, *J* = 2.5 Hz, 1H), 7.33 (d, *J* = 2Hz, 1H), 7.22-7.19 (dd, *J* = 7.5, 6 Hz, 2H), 5.57 (s, 2H), 2.29 (s, 3H), 1.49 (s, 9H), 1.23 (s, 9H).

3.7.4. Crystallographic Data

Table 3.1: Crystallographic Parameters of $[H(^{DIPP}CC)][Co(PPh_3)Br_3]$.

Empirical formula	$C_{60}H_{70}N_2PCoBr_4$
Formula weight	1228.72
Temperature (K)	100.15
Crystal system	triclinic
Space group	P-1
a (Å)	13.5583(4)
b (Å)	14.9390(5)
c (Å)	15.0811(5)
α (°)	98.672(2)
β (°)	106.946(2)
γ (°)	90.344(2)
Volume (Å^3)	2884.57(16)
Z	1
Radiation	MoKα (λ = 0.71073)
Reflections collected	56581
Independent reflections	10618 [R_{int} = 0.0446]
Goodness-of-fit on F^2	1.075
Final R indexes [I>=2σ (I)]	R_1 = 0.0622 wR_2 = 0.1557
Final R indexes [all data]	R_1 = 0.0769 wR_2 = 0.1700

3.8 References

1. Chianese, A. R.; Mo, A.; Lampland, N. L.; Swartz, R. L.; Bremer, P. T. Iridium Complexes of CCC-Pincer Ligands: Synthesis and Catalytic C—H Functionalization. *Organometallics*. **2010**, *29*, 3019−3026.
2. Ibrahim, A. D.; Tokmic, K.; Brennan, M. R.; Kim, D.; Matson, E. M.; Nilges, M. J.; Bertke, J. A.; Fout, A. R. Monoanionic Bis(Carbene) Pincer Complexes Featuring Cobalt(I-III) Oxidation States. *Dalton Trans* **2016**, *45* (24), 9805–9811.
3. Tokmic, K.; Markus, C. R.; Zhu, L.; Fout, A. R. Well-Defined Cobalt(I) Dihydrogen Catalyst: Experimental Evidence for a Co(I)/Co(III) Redox Process in Olefin Hydrogenation. *Journal of the American Chemical Society* **2016**, *138* (36), 11907.
4. Ibrahim, A. D.; Entsminger, S. W.; Zhu, L.; Fout, A. R. A Highly Chemoselective Cobalt Catalyst for the Hydrosilylation of Alkenes Using Tertiary Silanes and Hydrosiloxanes. *ACS Catalysis* **2016**, *6* (6), 3589.
5. Martinez, G. E.; Ocampo, C.; Park, Y. J.; Fout, A. R. Accessing Pincer Bis(Carbene) Ni(IV) Complexes From Ni(II) via Halogen and Halogen Surrogates. *Journal of the American Chemical Society* **2016**, *138* (13), 4290.
6. Brennan, M. R., Kim, D., Fout, A. R. A Synthetic and Mechanistic Investigation into the Cobalt(I) Catalyzed Amination of Aryl Halide. *Chem*. *Sci*. **2014**, *5*, 4831-4839.
7. Dunina, V. V.; Gorunova, O. N. Phosphapalladacycles: Preparation Routes. *Russian Chemical Reviews.* **2004**, *73* (4), 309-350.
8. Zhang, H.; Liu, J.; Chen, J.; Zhao, J.; Zhao, Y.; Li, L. A Modified Procedure for the Synthesis of 1-Arylimidazoles. *Synthesis* **2003**, *17*, 2661.
9. Kawamura, K.; Fukuzawa, H.; Hayashi, M. Enantioselective Copper-Catalyzed 1,4-Addition of Dialkylzincs to Enones Followed by Trapping with Allyl Iodide Derivatives. *Bulletin of the Chemical Society of Japan* **2011**, *84* (6), 640.
10. Mike, C. A., Nelson, T., Graham, J., Cordes, A. W., Allison, N. T. Synthesis and Structures of Dibenzometallacyclohexa-2,5-dienes. *Organometallics.* **1998**, *7*, 2573-2575.
11. Mo, Z., Chen, D., Leng, X., Deng, L. Intramolecular C(sp^3)—H Bond Activation Reactions of Low-Valent Cobalt Complexes with Coordination Unsaturation. *Organometallics.* **2012**, *31*, 7040-7043.
12. Mo, Z.; Liu, Y.; Deng, L. Anchoring of Silyl Donors on a *N*-Heterocyclic Carbene Through the Cobalt-Mediated Silylation of Benzylic C—H Bonds. *Angew. Chem. Int. Ed.* **2013**, *52* (41), 10845-10849.
13. Yamaguchi, Y.; Kashiwabara, T.; Ogata, K.; Miura, Y.; Nakamura, Y.; Kobayashi, K.; Ito, T. Synthesis and Reactivity of Triethylborane Adduct of N-Heterocyclic Carbene: Versatile Synthons for Synthesis of N-Heterocyclic Carbene Complexes. *Chemical Communications* **2004**, *19*, 2160.
14. Nugent, J.; Espinosa Martinez, G.; Fout, A. R. *Submitted.*
15. Li, J., Li, X., Sun, H. Synthesis and Characterization of Novel Organonickel and Organocobalt Complexes via Carbon-chlorine Bond Activation*. J. Organomet. Chem*. **2013**, *743*, 114-122.
16. Raba, A.; Anneser, M. R.; Jantke, D.; Cokoja, M.; Herrmann, W. A.; Kühn, F. E. Facile and Scalable Preparation of 2-Imidazolylpyridines. *Tetrahedron Letters* **2013**, *54* (26), 3384.
17. Klein, H. F.; Karsch, H. H. Methyltetrakis(trimethylphospin)kobalt und seine Derivate. *Chem. Ber.* **1975**, *108*, 944-955.

18. Cotton, F. A.; Faut, O. D.; Goodgame, D. M. L.; Holm, R. H. Magnetic Investigations of Spin-free Cobaltous Complexes. VI.[1] Complexes Containing Phosphines and the Position of Phosphines in the Spectrochemical Series. *J. Am. Chem. Soc.* **1961**, *83* (8), 1780-1785.